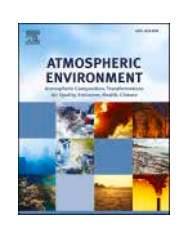
ELSEVIER

Contents lists available at ScienceDirect

Atmospheric Environment

journal homepage: www.elsevier.com/locate/atmosenv





A worldwide aerosol phenomenology: Elemental and organic carbon in $PM_{2.5}$ and PM_{10}

```
Jean-Philippe Putaud <sup>a,*</sup> , Fabrizia Cavalli <sup>a</sup>, Karl Espen Yttri <sup>b</sup>, Judith C. Chow <sup>c</sup>,
John G. Watson 6, Baerbel Sinha 6, Chandra Venkataraman 6, Fumikazu Ikemori f,ba 6,
Jean-Luc Jaffrezo<sup>8</sup>, Gaelle Uzu<sup>8</sup>, Isabel Moreno<sup>h,1</sup>, Radovan Krejci<sup>1</sup>, Paolo Laj<sup>1</sup>,
Tarun Gupta ko, Min Hu, Sang-Woo Kim o, Olga Mayol-Bracero ko, Patricia Quinn o,
Wenche Aas <sup>b</sup>, Andres Alastuey <sup>p</sup>, Marcos Andrade <sup>h</sup>, Monica Angelucci <sup>q,2</sup>, Gupta Anurag <sup>e</sup>,
J. Paul Beukes<sup>r</sup>, Ankur Bhardwaj<sup>s</sup>, Abhijit Chatterjee<sup>t</sup>, Pooja Chaudhary<sup>c</sup>
Anil Kumar Chhangani<sup>u</sup>, Sébastien Conil<sup>v</sup>, Anna Degorska<sup>w</sup>, Sandeep Devaliya<sup>s</sup>,
Abisheg Dhandapani<sup>x</sup>, Sandeep Singh Duhan<sup>y</sup>, Umesh Chandra Dumka<sup>z,bb</sup>, Gazala Habib<sup>aa</sup>,
Zahra Hamzavi<sup>1</sup>, Diksha Haswani<sup>8</sup>, Hartmut Herrmann<sup>ab</sup>, Adela Holubova<sup>ac</sup>,
Christoph Hueglin ad, Mohd Imran aa, Arshid Jehangir ee,
Taveen Singh Kapoor <sup>e</sup>, Angeliki Karanasiou <sup>p</sup>, Ravindra Khaiwal <sup>af</sup>
Jeongeun Kim <sup>ag</sup>, Tanja Kolesa <sup>ah</sup>, Joanna Kozakiewicz <sup>ai</sup>, Irena Kranjc <sup>ah</sup>, Jitender Singh Laura <sup>y</sup>,
Yang Lian <sup>aj</sup> , Junwen Liu <sup>ak</sup>, Pooja Manwani <sup>e</sup>, Valeria Mardoñez-Balderrama <sup>g,h,3</sup>
Béatrice Marticorena <sup>al</sup> , Atsushi Matsuki <sup>am</sup> , Suman Mor <sup>an</sup>, Sauryadeep Mukherjee <sup>t</sup>,
Sadashiva Murthy <sup>ao</sup>, Akila Muthalagu <sup>ap</sup>, Tanveer Ahmad Najar <sup>ae</sup>,
Radhakrishnan Naresh Kumar <sup>x</sup>, Govindan Pandithurai <sup>aj</sup>, Noemi Perez <sup>p</sup>,
Worradorn Phairuang aq, ar [0], Harish C. Phuleria e,
Laurent Poulain abo, Laxmi Prasad o, Delwin Pullokaran o, Adnan Mateen Qadri k,
Asif Qureshi <sup>ap</sup>, Omar Ramírez <sup>as</sup>, Sayantee Roy <sup>aa</sup>, Julian Rüdiger <sup>at</sup>, Binoy K. Saikia <sup>au</sup>,
Prasenjit Saikia <sup>au</sup>, Stéphane Sauvage <sup>av</sup>, Chrysanthos Savvides <sup>aw</sup>, Renuka Sharma <sup>e</sup>,
Tanbir Singh an, Gyanesh Kumar Singh k, Ronald Spoor ax o, Atul Kumar Srivastava ay,
Ramya Sunder Raman <sup>8</sup>0, Pieter G. Van Zyl <sup>r</sup>0, Marco Vecchiocattivi <sup>q</sup>, Céline Voiron <sup>8</sup>,
Jinyuan Xin az, Kajal Yadav o
```

E-mail address: Jean.PUTAUD@ec.europa.eu (J.-P. Putaud).

^a European Commission, Joint Research Centre (JRC), Ispra, Italy

^b NILU, Kjeller, Norway

^c Division of Atmospheric Sciences, Desert Research Institute, Reno, NV, USA

d Department of Earth and Environmental Sciences, Indian Institute of Science Education and Research Mohali, Sector 81, S.A.S Nagar, India

^e Interdisciplinary Program in Climate Studies, Indian Institute of Technology Bombay, Maharashtra, India

^f Nagoya city Institute for Environmental Sciences, Nagoya, Japan

g Institut des Géosciences de l'Environnement, Université Grenoble Alpes, CNRS, IRD, Grenoble INP, France

h Laboratorio de Física de la Atmósfera, Instituto de Investigaciones Físicas, Universidad Mayor de San Andrés, La Paz, Bolivia

¹ Department of Environmental Science & Bolin Centre for Climate Research, Stockholm, Sweden

^j World Meteorological Organization (WMO), Geneva, Switzerland

^k Department of Civil Engineering, Indian Institute of Technology Kanpur, Kanpur, India

State Key Laboratory of Regional Environment and Sustainability, College of Environmental Sciences and Engineering, Peking University, Beijing, China

^m School of Earth and Environmental Sciences, Seoul National University, Seoul, South Korea

ⁿ Brookhaven National Laboratory, Upton, NY, USA

o National Oceanic and Atmospheric Administration (NOAA) Pacific Marine Environmental Laboratory (PMEL), Seattle (WA, USA

 $^{^{\}rm p}$ Institute of Environmental Assessment and Water Research (IDAEA-CSIC), Barcelona, Spain

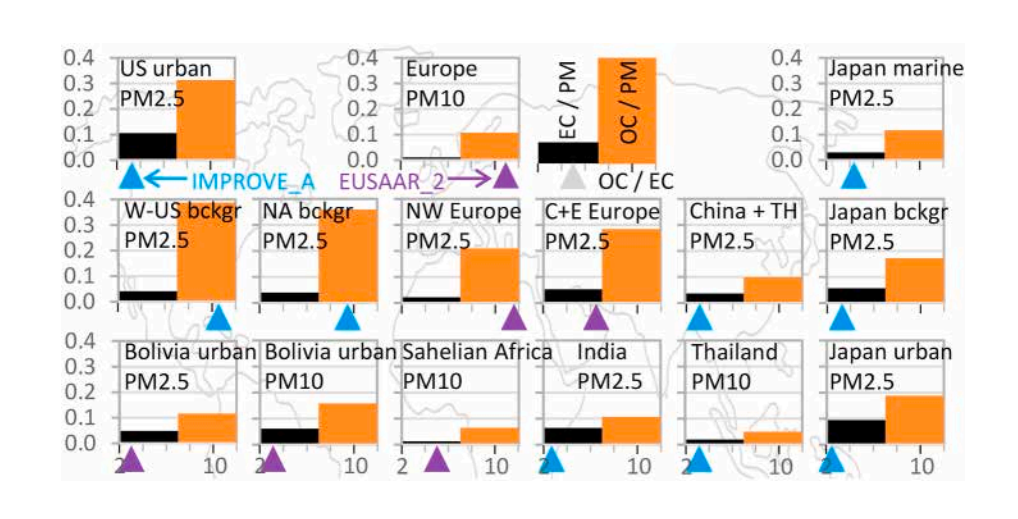
^{*} Corresponding author.

- ^q Agenzia Regionale per la Protezione Ambientale dell'Umbria, Perugia, Italy
- ¹ Atmospheric Chemistry Research Group, Chemical Resource Beneficiation, North-West University, Potchefstroom, South Africa
- s Department of Earth and Environmental Sciences, Indian Institute of Science Education and Research Bhopal, Bhopal, India
- ^t Department of Chemical Sciences, Bose Institute, Salt Lake, Kolkata, India
- ^u Department of Environmental Science, Maharaja Ganga Singh University, Bikaner, India
- v Observatoire Pérenne de l'Environnement, DISTEC/EES, ANDRA, Bure, France
- w Institute of Environmental Protection National Research Institute, Warsaw, Poland
- ^x Department of Civil and Environmental Engineering, Birla Institute of Technology Mesra, Ranchi, India
- y Environmental Sciences, Maharshi Dayanand University, Haryana, India
- ² Aryabhatta Research Institute of Observational Sciences (ARIES), Nainital, India
- ^{aa} Department of Civil Engineering, Indian Institute of Technology Delhi, New Delhi, India
- ab Leibniz Institute for Tropospheric Research, Atmospheric Chemistry Department (ACD), Leipzig, Germany
- ^{ac} Czech Hydrometeorological Institute, Air Quality Department, Prague, Czech Republic
- ad EMPA, Laboratory for Air Pollution and Environmental Technology, Dübendorf, Switzerland
- ae Department of Environmental Science, School of Earth and Environmental Sciences, University of Kashmir, Srinagar, India
- af Department of Community Medicine & School of Public Health, Post Graduate Institute of Medical Education & Research (PGIMER), Chandigarh, India
- ^{ag} National Institute of Meteorological Sciences, Seogwipo, South Korea
- ^{ah} Slovenian Environment Agency, Ljubljana, Slovenia
- ^{ai} Chief Inspectorate for Environmental Protection, Warsaw, Poland
- ^{aj} Indian Institute of Tropical Meteorology Pune, Pune, India
- ak College of Environment and Climate, Institute for Environmental and Climate Research, Jinan University, Guangzhou, China
- ^{al} Université Paris Est Créteil, Université Paris Cité, CNRS, LISA, Paris, France
- ^{am} Institute of Nature and Environmental Technology, Kanazawa University, Kanazawa, Japan
- an Department of Environment Studies, Panjab University, Chandigarh, India
- ao Department of Environmental Engineering, SJCE, JSS Science and Technology University, Mysore, India
- ^{ap} Department of Civil Engineering, Indian Institute of Technology Hyderabad, Kandi, India
- aq Department of Geography, Faculty of Social Sciences, Chiang Mai University, Chiang Mai, Thailand
- ar Faculty of Geosciences and Civil Engineering, Institute of Science and Engineering, Kanazawa University, Kanazawa, Japan
- ^{as} Universidad Militar Nueva Granada, Cajicá, Colombia
- ^{at} Air Monitoring Network, German Environment Agency / Umweltbundesamt, Langen, Germany
- ^{au} Coal & Energy Division, CSIR-North East Institute of Science and Technology, Jorhat, India
- av CERI EE IMT Nord Europe Centre for Energy and Environment, Douai, France
- ^{aw} Air Quality Section, Department of Labour Inspection, Ministry of Labour and Social Insurance, Nicosia, Cyprus
- ^{ax} National Institute for Public Health and the Environment, Bilthoven, Netherlands
- ^{ay} Indian Institute of Tropical Meteorology, Ministry of Earth Sciences, New Delhi, India
- az State Key Laboratory of Atmospheric Environment and Extreme Meteorology, Institute of Atmospheric Physics, Chinese Academy of Sciences, Beijing, China
- ba Graduate School of Integrated Science and Technology, Nagasaki University, Nagasaki, Japan
- bb Department of Physics, Graphic Era (Deemed to be University), Dehradun, India

HIGHLIGHTS

- The carbon content of atmospheric particulate matter (PM) worldwide is assessed.
- Data from hundreds of sites in Africa, Asia, America, and Europe are compared.
- Organic carbon/PM ratios are highest in North America.
- Elemental carbon/PM ratios are highest at urban sites.
- Organic carbon/Elemental carbon ratios are highest in North America and Europe.

G R A P H I C A L A B S T R A C T



ABSTRACT

Elemental carbon (EC), organic carbon (OC), and particulate matter (PM) concentrations in the inhalable (PM₁₀) and fine (PM_{2.5}) size fractions are measured worldwide, albeit with different analytical methods. These measurements from many researchers were collected and analyzed for Africa, America, Asia, and Europe

 $^{^{1}}$ Now at: Instituto de Investigaciones Fármaco Bioquímicas, Universidad Mayor de San Andrés, Av. Saavedra N 2224, La Paz, Bolivia.

² Now at: Regione Umbria, Perugia, Italy.

³ Now at: Institute for Atmospheric Sciences and Climate, National Research Council of Italy, CNR-ISAC, Bologna, Italy.

for 2012–2019. EC/PM, OC/PM, and OC/EC ratios were examined based on region, site type, and season to infer potential sources and impacts. These analyses demonstrate that carbonaceous materials are important PM constituents throughout the world. Mean EC/PM ratios were lowest in PM_{10} in Sahelian Africa and Europe (\sim 0.01), highest (>0.07) in $PM_{2.5}$ at urban sites in North America, South America, and Japan. Mean OC/PM ratios were lowest in PM_{10} in the Sahel (\sim 0.06) and in $PM_{2.5}$ in China and Thailand (0.10), and highest in central and eastern Europe (\sim 0.3) and North America (\sim 0.4). OC/EC ratios were elevated in western and northern Europe, and at regional background sites in North America. EC/PM increased with PM_{10} in Thailand, while OC/PM increased with higher PM mass in Thailand, India, and North America, highlighting the specific contribution of carbonaceous aerosols to PM pollution in these regions. At European and North American background sites, OC/EC ratios increased with PM mass. Higher OC/EC ratios in dry periods indicate influence of wildfires, prescribed burns, and secondary aerosol formation. Elevated wintertime EC/PM ratios coincide with residential heating in temperate climate zones.

1. Introduction

The inhalable fraction of airborne particulate matter (PM₁₀), and especially its fine fraction (PM_{2.5}), is recognized as threats to human health (Atkinson et al., 2014; Beelen et al., 2014; Lee et al., 2015; Li et al., 2022; US-EPA, 2019). Combustion particles, containing mostly elemental carbon (EC) and organic carbon (OC), have been identified as disproportionately harmful (Lewtas, 2007; Shiraiwa et al., 2012; Tang et al., 2024). However, the specific factors driving the toxicity of particulate pollution are still uncertain (Schtaufnagel, 2020; Thangavel et al., 2022). Airborne particles also play a climatic role through their scattering and absorption of solar radiation, and as cloud condensation nuclei (Chen et al., 2018; Lohman et al., 2020; Thornhill et al., 2021). Particulate matter (PM) health and climate effect both depend on particle size and chemical composition.

While PM components including sulfate, nitrate, ammonium, and elements ranging from sodium to uranium can be accurately identified and measured, carbonaceous compounds are so various and numerous that only a limited fraction of them are quantifiable or even identified with current molecular analytical techniques (Johnston and Kerecman, 2019). However, total carbon (TC) content and operationally defined sub-fractions such as OC and EC can be quantified by thermal techniques (Watson et al., 2005). EC is a primary pollutant emitted as solid black particles from incomplete combustion processes. Specific EC health impacts (morbidity and mortality) and possible mechanisms were recently listed by Hang et al. (2023). In the atmosphere, internally and externally mixed EC particles absorb light, contributing to climate warming (Kelesidis et al., 2022). In contrast, particulate OC does not come only from combustion processes, but also from natural biogenic sources and from the photochemical conversion of organic gases to particles. Particulate organic matter can contain toxic substances such as carcinogenic polycyclic aromatic hydrocarbons and quinones (Bolton et al., 2000). Globally, OC is currently believed to cause negative radiative forcing (Szopa et al., 2023). However, some organic materials, such as those from the smoldering phase of biomass burning and secondary aerosol production, absorb more visible light at wavelengths shorter than 500 nm (Zhang et al., 2020), and this "brown carbon" can cause positive radiative forcing. An OC coating of an EC core can also result in a lensing effect that enhances EC light absorption (Zhang et al., 2018).

A 2019 global emission inventory found major EC emission contributors from the residential sector (30 %), industries (24 %), transportation (18 %), and biomass burning (9 %), with a total annual emission of 5 TgC/yr (EDGAR, 2024). In comparison, primary anthropic global OC emissions were estimated at 11 TgC/yr (EDGAR, 2024), mainly from the residential sector (48 %), biomass burning (27 %), industries (15 %), and transportation (4 %). Emissions from natural sources remain uncertain. Leon-Marcos et al. (2024) estimated global OC emissions from the sea surface microlayer to range between 6 and 17 TgC/yr. Additionally, Samaké et al. (2020) estimated global terrestrial primary biogenic organic aerosol (PBOA) emissions at 50 to 1000 Tg/yr. An important part of PBOA particles could be larger than 10 μ m. However, PBOA contributions to PM₁₀ were reported by Bozzetti et al. (2016) and Yttri et al. (2021). Particulate OC is also produced through atmospheric reactions yielding condensable organic species from

volatile and semi-volatile precursors. Estimates of global secondary organic aerosol (SOA) production range from 12 to 1820 Tg/yr (Kelly et al., 2018). Hallquist et al. (2009) estimated a global SOA flux of 115 TgC/yr, primarily derived from biogenic (75 %), biomass burning (15 %), and anthropogenic (10 %) precursors. OC and EC sources are variable in time and space, resulting in large spatial and temporal variations in particulate OC and EC concentrations.

A recent meta-analysis of OC and EC data compiled from 625 worldwide datasets and several PM size fractions found OC and EC concentration differences between rural and highly-trafficked areas, as well as the dependence of OC/EC ratios on the PM size fraction (Fakhri et al., 2024). The current study focuses on the carbonaceous content of PM_{10} and $PM_{2.5}$ over the period 2012–2019, as described by the EC/PM, OC/PM and OC/EC ratios. Such ratios are less dependent on source strengths and pollution dispersion than atmospheric concentrations and can be related to emission sources and atmospheric processes leading to the observed PM concentrations and composition. They are also crucial metrics for constraining regional and global models that aim to describe human exposure to inhalable carbonaceous PM, as well as the impact of carbon-containing particles on climate. The dependence of PM carbon content on seasons and PM mass concentrations is first analyzed for each of the world regions from which relevant data were collected. The OC and EC data used in this study (Fig. 1) were all obtained from thermal-optical analyses, albeit employing different analytical protocols. Data were eventually harmonized (Section 3.5) to account for differences between the various methods.

2. Experimental

2.1. Data collection

The sites from which data were used are shown in Fig. 1 and listed in Table S1. Ninety percent (90 %) of the PM₁₀, PM_{2.5}, OC and EC mass concentration data was obtained from open access databases. Data from 174 sites in North America and the Caribbean were downloaded from the Interagency Monitoring of Protected Visual Environments (IMPROVE) network web site (vista.cira.colostate.edu/Improve). Data from 28 European sites were accessed via the Aerosol, Clouds and Trace Gases Research Infrastructure (ACTRIS) Data Center at ebas-data.nilu. no. Data from 110 sites in Japan were downloaded from the Japanese Ministry of Environment web site (www.env.go.jp, in Japanese), except for the Noto site, for which data were provided by its originator. Data from four west and central African sites were downloaded from the International Network to study Deposition and Atmospheric composition in Africa (INDAAF) web site (indaaf.obs-mip.fr/catalogue), whereas data from South Africa were provided by their originator. Large parts of the world are not covered by open access databases. Data sets from these regions were identified by members of the WMO-GAW-SAG-Aerosol (World Meteorological Organization-Global Atmospheric Watch-Scientific Advisory Group). Data from 4 sites in South America were made available by the data originators, as were data from 9 sites in China, 14 sites in India, and 3 sites in both South Korea and Thailand. All data used in this study are available at zenodo.org/uploads/14036033, except for data from boreal Africa, North America and Europe, which are easily accessible from the web sites listed above.

Data sets were deemed representative for the actual sites when measurements covered at last one year, with at least ten data points per season.

2.2. Measurements

The data used in this study primarily comes from off-line analyses of particulate matter (PM) collected on quartz fiber filters. Measurements in PM_{10} and $PM_{2.5}$ were available for 23, and 335 sites, respectively. Data for both PM_{10} and $PM_{2.5}$ were collected from eight sites only (Table S1).

Data from Thailand were derived from the analysis of PM collected with a multi-stage impactor followed by a backup filter, as described by Phairuang et al. (2019). While low pressure drops in such an impactor likely limit negative sampling artefacts, positive artefacts affecting the sampling of PM by the back-up filter have been reported (Kuwabara et al., 2016). It is to be noted that OC and EC were not measured on the inertial filter of the impactor (0.1–0.5 μm) where the PM mass collected was generally (99th percentile) less than 10 % of the total sub-2.5 μm mass.

Filter sampling is prone to positive and negative artefacts (Chow et al., 2010; Maimone et al., 2011; Watson et al., 2009), affecting mainly the collection of semi-volatile species (e.g., NH_4NO_3 , semi-volatile organics). Such artefacts can cause an overestimation or underestimation of the actual particulate OC and total PM_{10} or $PM_{2.5}$ mass concentrations. There are no means to consistently account for these artefacts in this study. Therefore, they were disregarded in our analysis, which is in line with the meaning of the term "phenomenology", being the study of appearances, as opposed to reality (Smith, 2018).

2.2.1. OC and EC measurements

In PM carbonaceous content thermal analyses, the carbon released by the sample by volatilization (in an inert gas) is considered to be OC, while the remaining carbon that combusts in an oxidizing atmosphere is assigned to EC. Carbonate carbon can evolve as OC and/or EC depending on carbonate structure, grain size, and the thermal protocol applied. This simple method is complicated by OC charring in the inert atmosphere that can positively bias the EC concentration. This is compensated by monitoring reflected (R) and/or transmitted (T) light from a laser that quantifies darkening of the aerosol deposit during the inert

phase, with whitening during the oxidization phase. Pyrolyzed OC is determined as the carbon that evolves in the oxidation phase until R and/or T achieve their initial values; carbon evolving after this is classified as EC. The OC/EC split depends on the temperature protocol, and time spent at each temperature plateau, and whether the pyrolysis correction is determined by T or R. EC determined by reflectance can be twice EC determined by transmittance. Chow et al. (2004) attributed this discrepancy to charring of adsorbed organic vapors within the quartz filter that affect transmittance more than reflectance that is dominated by charring of particle deposits on the filter surface. Since OC is the major fraction of TC, the correction is not as large as it is for EC. Differences between the various thermal-optical protocols used to determine OC and EC were discussed by Karanasiou et al. (2015). To enable comparisons in Section 3.5, OC and EC data obtained using these different methods were harmonized, as described in Section 2.3.

Table S1 identifies the different thermal-optical protocols applied to the acquired data sets. Data from most sites in Africa, from South America, and from Europe were produced using the EUSAAR_2 protocol (Cavalli et al., 2010) that uses transmittance corrections. Data from North America and most sites in Asia were obtained using the IMPRO-VE_A protocol (Chow et al., 2007), which reports both reflectance and transmittance corrections, but accepts the reflectance EC values for reporting. Data from four of the Asian sites result from semi-continuous OC and EC monitors following a NIOSH-5040-like protocol (Peterson and Richards, 2002) with a transmittance correction.

OC, EC, and PM $_{2.5}$ mass concentrations from North American IMPROVE sites have been consistently measured by the same laboratories (Desert Research Institute for carbon and University of California at Davis for mass) since 1986. More than $^3\!\!/$ of the sites in India are part of the COALESCE (Carbonaceous Aerosol Emissions, Source Apportionment and Climate Impacts) network (Venkataraman et al., 2020), which ensures data quality. Data from Europe and most sites in Africa and South America, were produced by laboratories that participate in annual inter-laboratory comparisons (ILC) to ensure data quality. Recent ILC exercises showed a reproducibility of about 5 % for Total Carbon (TC = OC + EC) and about 10 % for the EC/TC ratio. Comparable levels of uncertainties can be expected for data from other sites, mainly located in eastern Asia.

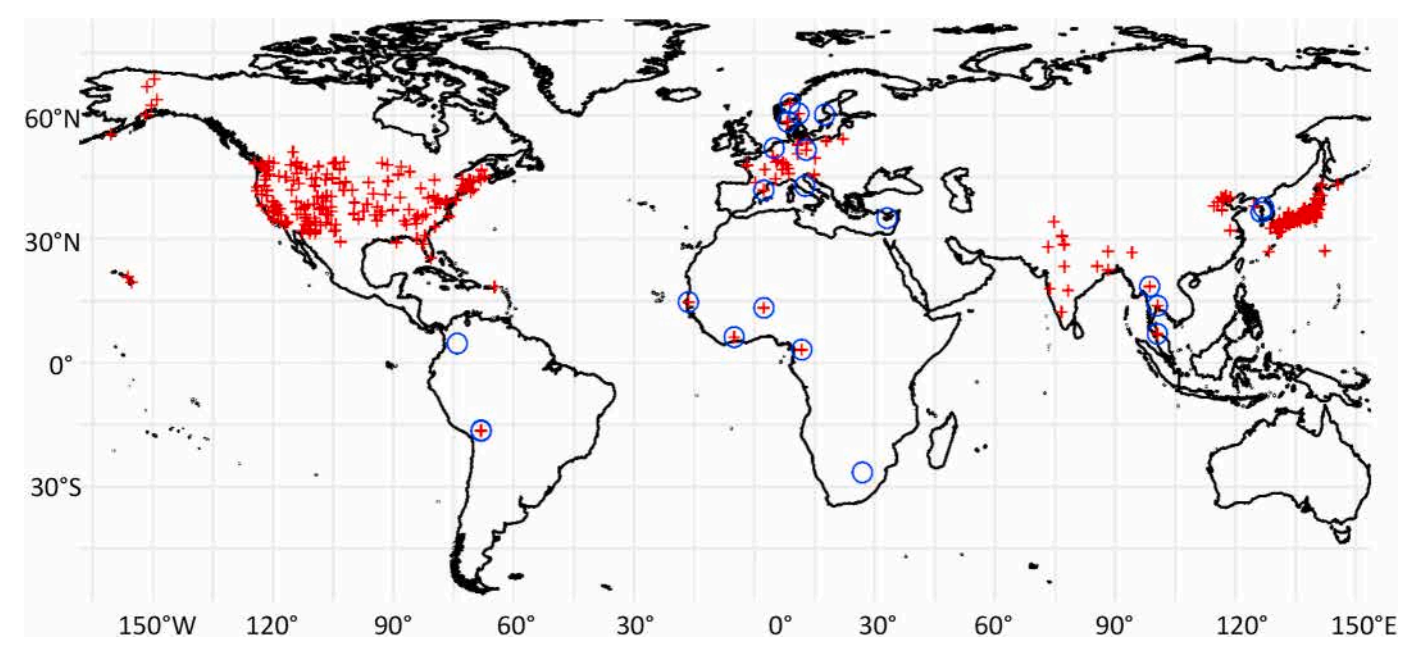


Fig. 1. Location of the sites from which OC, EC, and PM mass data in PM_{2.5} (crosses) and PM₁₀ (circles) were selected.

2.2.2. Total mass concentrations measurements

PM mass measurements were mostly performed by gravimetric analysis, except for 18 sites in Africa, Asia and Europe that used continuous β -Ray Attenuation Monitors, Tapered Element Oscillating Microbalance – with or without Filter Dynamic Measurement System), or Optical Particle Counter, as listed in Table S1. The equivalence of these automatic devices with the gravimetric method has been examined (Waldén et al., 2010).

2.3. Data processing

Data from continuous monitors were averaged over 24 h for comparison with the filter measurements. Concentrations were converted to standard pressure and temperature conditions. Samples with PM mass less than $0.2\,\mu\text{g/m}^3$ or OC and/or EC concentrations less than $0.1\,\mu\text{g/m}^3$ were excluded from statistical analyses, unless otherwise specified. Samples where OC + EC was greater than PM were also rejected. PM_{10} and $PM_{2.5}$ data from Thailand were calculated by summing the concentrations measured on the relevant stages of the impactor.

EC/PM, OC/PM, and OC/EC ratios for $PM_{2.5}$ and PM_{10} were calculated for each sample. These ratios were averaged into PM mass concentration bins of constant width on a logarithmic scale. Bin boundaries started from $1.10~\mu g/m^3$ and included $6.25, 8.84, 12.5, 17.7, 25.0, 35.4, 50.0, 70.7, 100, 141, and <math>200~\mu g/m^3$. Averages were considered representative if they were calculated from at least five entries. The variability of PM concentrations and ratios within the bins were assessed using the 16th and the 84th percentiles, corresponding to one standard deviation in a Gaussian distribution. Seasonal variations in EC/PM, OC/PM, and OC/EC ratios were assessed by calculating averages over December to February (DJF), March to May (MAM), June to August (JJA), and September to November (SON), or monthly averages when sufficient data were available (i.e. more than five data points per month and PM mass range).

Conversion factors were estimated from comparisons of EUSAAR_2/T, IMPROVE_A/R, and NIOSH5040/T protocols applied to samples from Egbert, CA, Ispra, IT (Fig. S1), and various locations across the world (Bautista et al., 2015; Cheng et al., 2014; Yubero et al., 2014). The ratios between the OC and EC values determined using the different methods (Table S2) were arithmetically averaged. Given the variability of the values observed across the world, the uncertainty of the conversion factors (Table 1) is approximately \pm 30 %.

3. Results and discussion

3.1. Africa

3.1.1. OC and EC in PM_{10}

 PM_{10} mass concentrations from the four African sites (Table S1) – Bambey (SN), Banizoumbou (NE), Lamto (CI), and Welgegund (ZA) – ranged from <10 μ g/m 3 to ~ 100 μ g/m 3 (Welgegund) or more. Data from Bambey and Banizoumbou, both in the Sahel biogeographical region, were deemed similar enough (Fig. S2) to be averaged as "Sahel" (Fig. 2). The contributions of carbonaceous species to PM_{10} are on average much higher in Lamto, CI (equatorial Africa) and Welgegund, ZA (austral tropical Africa) than in the Sahel area. EC/PM and OC/PM ratios generally both decrease with increasing PM_{10} mass concentrations, indicating that carbonaceous aerosol are not primarily responsible

Table 1
Conversion factors for EC and OC for EUSAAR_2/T, IMPROVE_A/R, and NIOSH5040/T.

Thermal-optical methods	EC	OC
IMPROVE_A/EUSAAR_2	1.27	0.89
EUSAAR_2/NIOSH-5040	1.33	0.93
IMPROVE_A/NIOSH-5040	1.28	0.87

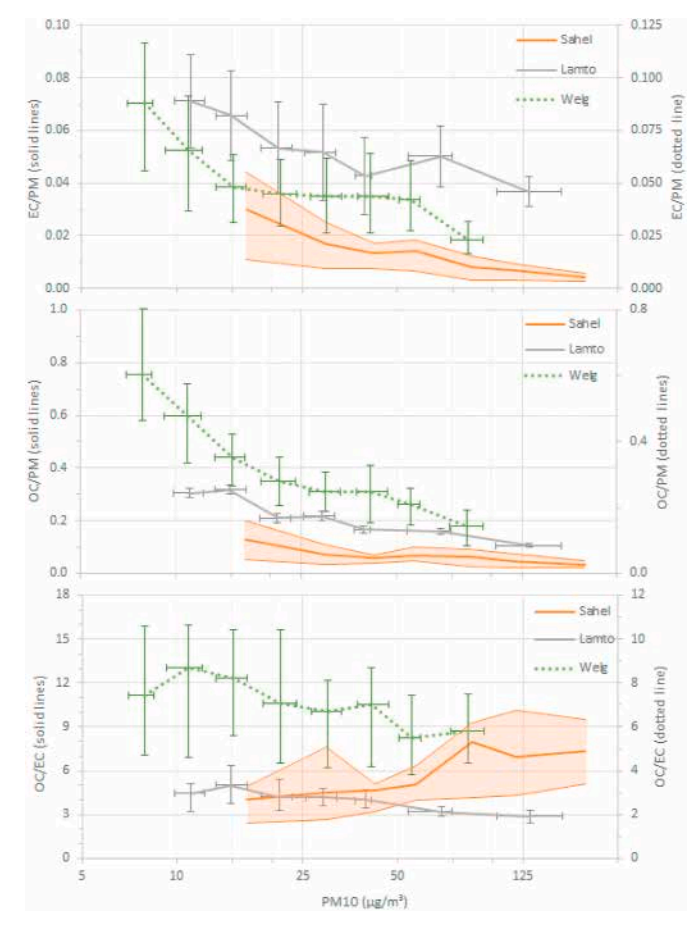


Fig. 2. EC/PM, OC/PM and OC/EC in PM₁₀ vs PM₁₀ mass at 3 locations in Africa. Measurements were performed with a different thermal protocol at Welgegund, and cannot be directly compared with others. Shaded areas and error bars show 16th and 84th percentiles.

for the high PM_{10} concentrations observed at these African sites. OC/EC ratios increase with PM_{10} mass up to concentrations of ${\sim}80~\mu g/m^3$ at the Sahel sites, and level off beyond. In contrast, OC/EC ratios in Welgegund (ZA) and Lamto (CI) decrease with increasing PM_{10} concentrations in the ranges $11{-}55~\mu g/m^3$ and $15{-}130~\mu g/m^3$, respectively (Fig. 2).

While no clear seasonal patterns are detected in OC/PM ratios, lower EC/PM ratios are observed in spring at all African sites (Fig. 3). This results in OC/EC seasonal cycles in ratios in the Sahel, with higher values in MAM, and lower values during JJA. In Sahelian Africa, the dry season extends from November to April-June, and is characterized by dry and dusty winds blowing from the Sahara, and biomass burning (Amoako and Gambiza, 2021). However, lower EC/PM₁₀ ratios in DJF and MAM suggest that combustion processes are not major sources of PM₁₀ during the dry season, while suspension of soil dust contributes coarse particles during this period (Kaly et al., 2015; Mahowald et al., 2024; Marticorena et al., 2017). At Lamto (CI), EC/PM₁₀ are higher in JJA, when PM concentrations are low due to wet removal, while black carbon emissions are attributed to domestic activities (Kouassi et al., 2021). OC/EC ratios are lower than in the Sahel in DJF and MAM, which could be explained by a major contribution of biomass burning in the savanna area on the edge of the African semi-deciduous forest (Ossohou et al., 2019). Even lower OC/EC ratios were observed by Ouafo-Leumbe et al. (2018) in the wet savanna of Benin. In Welgegund (ZA), a clear seasonal cycle of OC/EC ratios is observed, with a maximum in DJF (summer) and a minimum in JJA (winter), suggesting that the formation of SOA (favored in summer) is an important OC source at this site.

At all four African sites, high PM_{10} concentrations and low EC/PM and OC/PM predominantly occur during the dry winter season. This

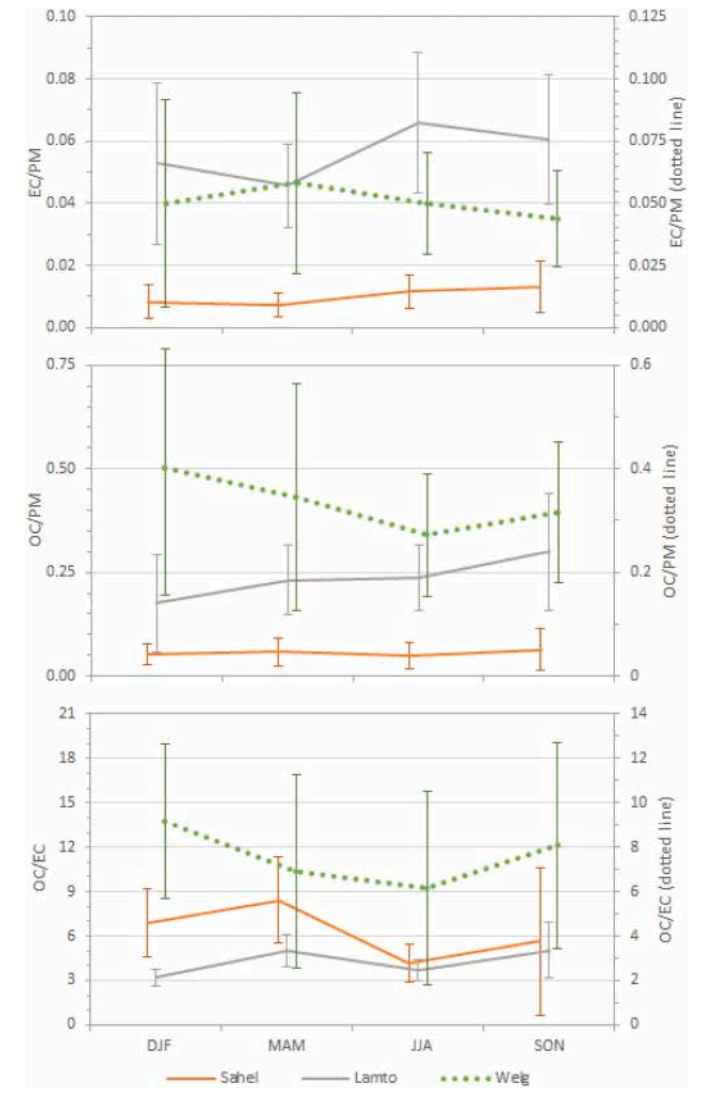


Fig. 3. Seasonal variations in the EC/PM, OC/PM and OC/EC ratios in PM_{10} at 3 locations in Africa. Measurements were performed with a different thermal protocol at Welgegund, and cannot be directly compared with others. Error bars represent 16th and 84th percentiles.

indicates that carbonaceous aerosol is not the main responsible for elevated PM_{10} concentration even during the biomass burning period, probably due to increased soil dust emissions during this time.

3.1.2. Mass size distribution of EC and OC across $PM_{2.5}$ and PM_{10}

 $PM_{2.5}$ mass concentration measurements were not available at the African sites. However, OC and EC were measured also in the $PM_{2.5}$ size fraction at Bambey (SN), Banizoumbou (NE), Lamto (CI), and Zoétélé (CM). On average, $EC(PM_{2.5})/EC(PM_{10})$ ratios were significantly (99.9 % confidence level) smaller than 1 at Bambey, Banizoumbou, and

Zoétélé, suggesting the presence of EC in the coarse aerosol fraction (PM $_{10}$ -PM $_{2.5}$) at these sites. OC(PM $_{2.5}$)/OC(PM $_{10}$) ratios were also significantly less than 1 and lower than the EC(PM $_{2.5}$)/EC(PM $_{10}$) ratios (99.9 % confidence level) at all four sites (Table 2), indicating the presence of OC and the enrichment of OC with respect to EC in the coarse aerosol. However, interferences with carbonate from mineral dust cannot be excluded. The decrease of OC(PM $_{2.5}$)/OC(PM $_{10}$) ratios with increasing PM $_{10}$ mass concentrations from PM $_{10}\approx30~\mu\text{g/m}^3$ (Fig. 4) is consistent with the hypothesis that increases in PM $_{10}$ mass concentrations are associated with increases in mineral dust, which may contain carbonates that would be detected as OC in thermal-optical analyses.

3.2. America

3.2.1. OC and EC in PM_{10}

 PM_{10} data were obtained from four high-altitude Andean sites in South America: Bogotá in Colombia (CO), and Chacaltaya, El Alto, and La Paz in Bolivia (BO). The data from the two neighboring urban sites (El Alto and La Paz) in Bolivia were deemed similar enough (Fig. S3) to be averaged and presented as Bolivia-U. PM mass concentration data points

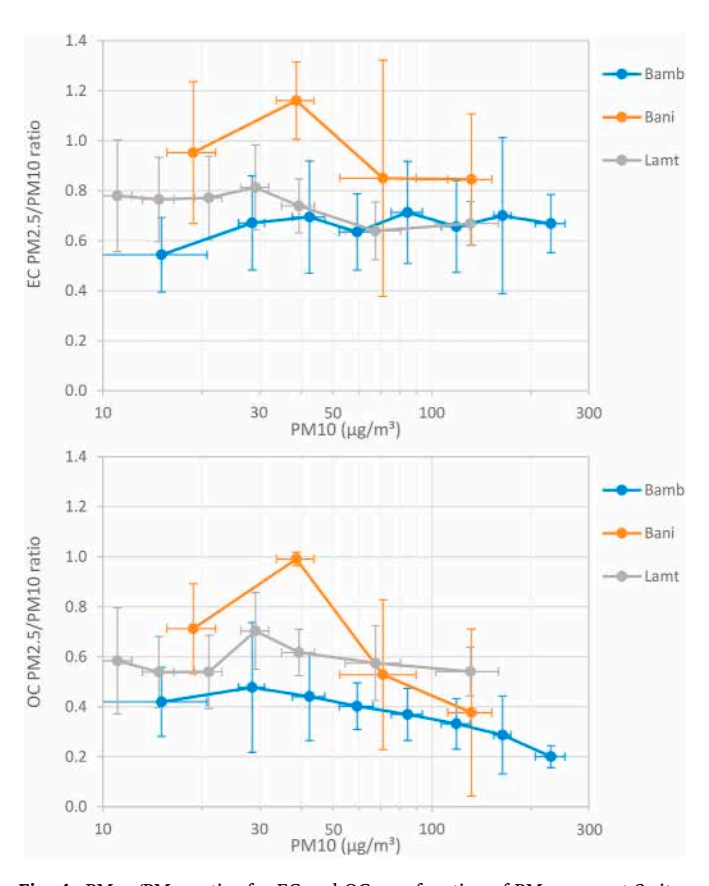


Fig. 4. $PM_{2.5}/PM_{10}$ ratios for EC and OC as a function of PM_{10} mass at 3 sites in Africa.

Table 2Contribution of the PM_{2.5} size fraction to the PM₁₀ size fraction for EC and OC at 4 African sites.

	PM _{2.5} /PM ₁₀ ratio								
			EC		OC				
	average	median	84th percentile	16th percentile	average	median	84th percentile	16th percentile	
Bambey	0.67	0.63	0.89	0.48	0.38	0.36	0.52	0.24	
Banizoumbou	0.85	0.77	1.19	0.61	0.56	0.50	0.96	0.21	
Lamto	0.75	0.76	0.94	0.59	0.58	0.58	0.71	0.42	
Zoétélé	0.71	0.69	1.00	0.45	0.52	0.46	0.79	0.25	

available from Chacaltaya were too few (5) to be included in the statistical analysis.

Both in Bogotá and at the urban sites in Bolivia, EC/PM $_{10}$ ratios generally decrease with increasing PM $_{10}$ mass concentrations, although the shape of the two curves differs (Fig. 5), suggesting different causes for these decreases. In contrast, OC/PM $_{10}$ ratios are independent of PM $_{10}$ concentrations between \sim 20 and 60 μ g/m 3 (Fig. 5). Consequently, OC/EC ratios increase with PM $_{10}$ mass concentrations up to \sim 60 μ g/m 3 in Bogotá, while they are independent from PM $_{10}$ concentrations above 30 μ g/m 3 at the Bolivia-U sites (Fig. 5).

However, PM_{10} concentrations greater than 50 μ g/m³ occurred only from January to April in Bogotá (CO) and from April to September at the Bolivia-U sites (Fig. 6). Therefore, the relationships between EC/ PM_{10} and PM_{10} concentrations also reflect seasonal variations because the right-hand tips of the curves in Fig. 5 correspond to data points in January to April and April to September in Bogotá and Bolivia-U, respectively. These seasonal variations are larger in Bogotá, especially for EC/ PM_{10} ratios (minimum in January to March) and OC/EC ratios (minimum in JJA), while at Bolivia-U sites, a clear seasonal cycle (maximum in August to November) can be observed for the OC/EC ratios only (Fig. 6).

Emissions from biomass burning and soil dust suspension both peak during the dry season, May to September in the Amazonian basin, and

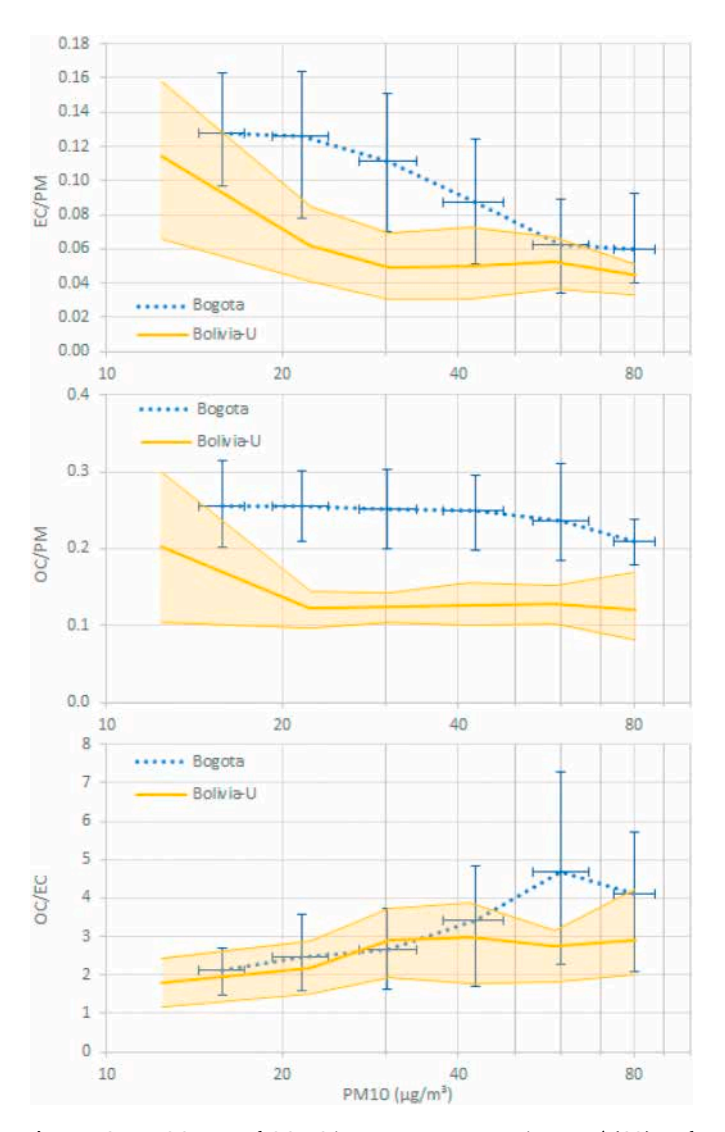


Fig. 5. EC/PM, OC/PM and OC/EC in PM_{10} vs PM_{10} mass in Bogotá (CO), and urban sites in Bolivia (Bolivia-U).

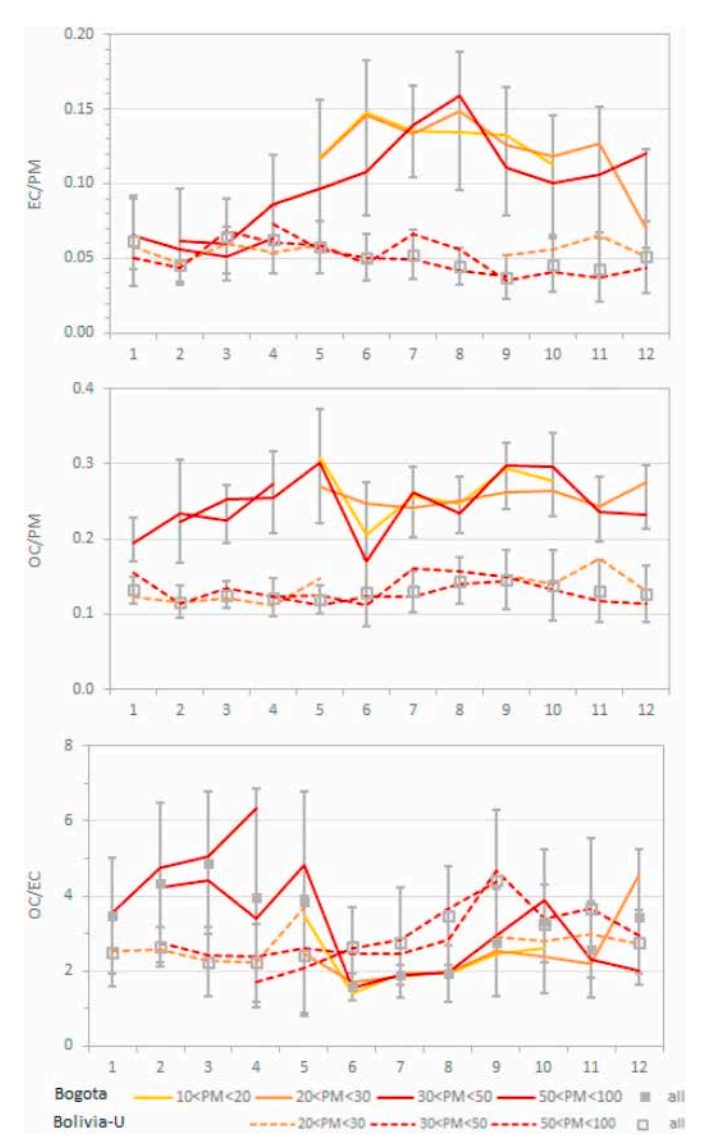


Fig. 6. Seasonal variations in EC/PM, OC/PM and OC/EC in PM_{10} at Bogotá (CO) and a pair of urban sites in Bolivia (Bolivia-U).

January to April in the tropical forest and savanna of northern South America (Mardoñez et al., 2023; Ramírez et al., 2018; Rincón-Riveros et al., 2020). These peaks correspond with the periods of high PM_{10} concentrations observed at the high-altitude urban sites in Bolivia and Colombia, respectively, suggesting that both soil dust and biomass burning emissions are responsible for higher PM_{10} mass concentrations. In Bogotá, the lowest EC/PM_{10} ratios observed from January to April could simply result from the increase of EC-free soil dust emissions. Biomass burning emissions being depleted in EC compared to other sources like traffic could also contribute. At the urban sites in Bolivia (Bolivia-U), EC/PM_{10} , OC/PM_{10} , or OC/EC are not significantly different during the whole dry season from May–September compared to the rest of the year.

At the mountain site of Chacaltaya (BO), annual mean OC and EC concentrations were 1.0 and 0.1 μ g/m³, respectively. Seasonal variations in the OC/EC ratio were calculated by selecting days on which EC concentrations were greater than 0.05 μ g/m³ (30th percentile) to limit uncertainties. They exhibit a minimum in MAM (Fig. S4), when longrange transport of OC from different sources is minimum (Moreno et al., 2024). Enhanced long-range transport of biomass burning emissions to Chacaltaya from August to November reported by Moreno et al. (2024) corresponds to the highest OC/EC ratios observed at the urban

sites in Bolivia.

In sum, PM_{10} air pollution in the Andean area of tropical South America is strongly associated with the dry season, during which biomass burning and soil dust emissions increase. This does not result in the enrichment of PM_{10} with carbonaceous matter. In Bogotá, the OC/EC ratio increases during the dry season (January–April) whereas in Bolivia higher OC/EC values are associated with pollution transport patterns rather than increased emissions during the dry season (May–September) in the Amazonian basin.

3.2.2. OC and EC in $PM_{2.5}$

Data from 173 sites in North America and one in the Caribbean (US Virgin Islands) were retrieved from the IMPROVE web site. OC and EC concentrations in $PM_{2.5}$ were also obtained from Chacaltaya, although without $PM_{2.5}$ mass data, El Alto, and La Paz (BO).

3.2.2.1. Caribbean Islands and Latin America. For the pair of urban sites El Alto and La Paz (Bolivia-U), the relationships between EC/PM $_{2.5}$, OC/PM $_{2.5}$, OC/EC, and PM $_{2.5}$ mass are similar to those observed for the PM $_{10}$ fraction. However, EC/PM and OC/PM are higher in the PM $_{2.5}$ fraction, especially at low PM concentrations (Fig. 7), probably due to a higher contribution of soil dust to the coarse fraction (PM $_{10}$ - PM $_{2.5}$). In the

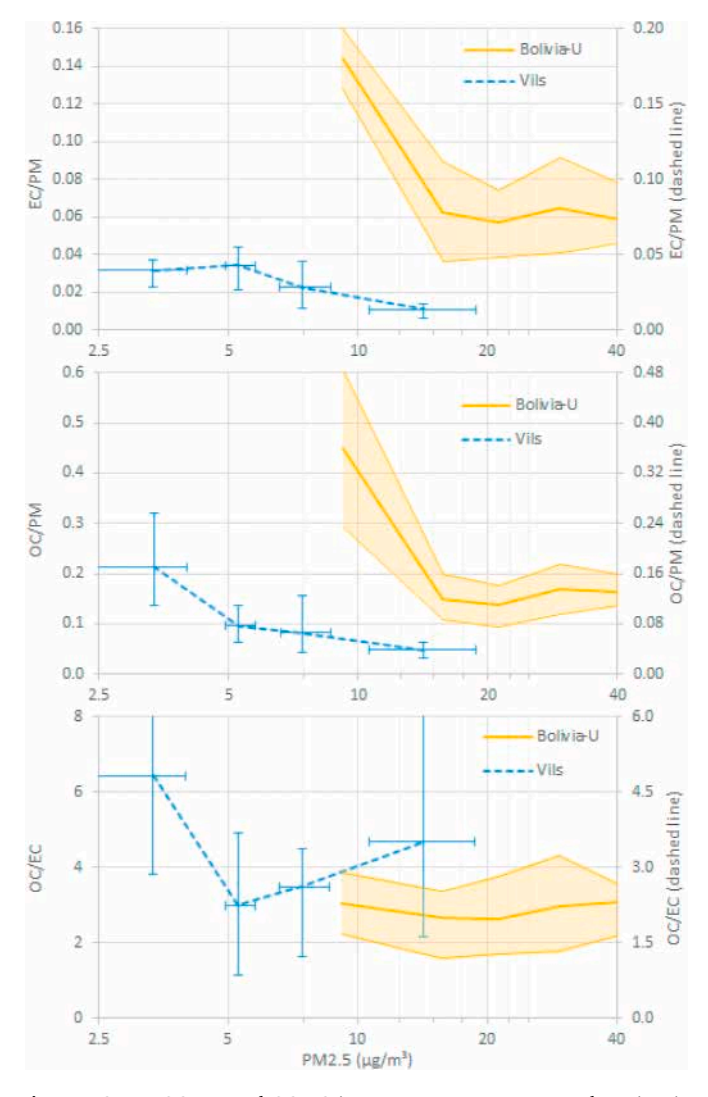


Fig. 7. EC/PM, OC/PM and OC/EC in $PM_{2.5}$ vs $PM_{2.5}$ mass at urban sites in Bolivia (Bolivia-U) and the US Virgin Islands in the Caribbean. Measurements were performed with different thermal protocols and cannot be directly compared.

Virgin Islands (ViIs), both EC/PM $_{2.5}$ and OC/PM $_{2.5}$ decrease with increasing PM $_{2.5}$ mass above 5 $\mu g/m^3$. In contrast, the OC/EC ratio increases with PM $_{2.5}$ above 5 $\mu g/m^3$. These observations are consistent with an increasing contribution of mineral dust with PM $_{2.5}$ mass concentrations in Bolivia. Higher OC/EC at very low PM $_{2.5}$ concentrations (1.5–4.5 $\mu g/m^3$) in the Caribbean Is could result from a higher contribution of primary marine organics or long-range transported pollution from continents.

3.2.2.2. North America. The relationships between the EC/PM, OC/PM, and OC/EC ratios and PM_{2.5} mass were examined for each site (Fig. S5) located in North America. These relationships appeared to be consistent across most sites except for three in the western USA, and at seven urban sites in the remainder of North America. The Puget Sound (PUSO) site (see Table S1) in the west was pooled with the seven urban sites.

For the ensemble of 75 regional background sites in the western USA, the EC/PM ratio decreases with PM $_{2.5}$ mass increasing from 1 to ${\sim}10\,\mu\text{g}/$ m^3 (Fig. 8), and increases with PM_{2.5} mass ranging from ~40 μ g/m³ up to $\sim 80~\mu g/m^3$. High EC/PM ratios at low PM_{2.5} concentrations could correspond to rainy days, while large EC/PM at high PM2.5 levels could result from the advection of pollution plumes from nearby combustion sources, including wildfires. Particularly high EC/PM ratios were observed at two sites in the western USA: Tahoe Lake (LTCC), CA, in the Sierra Nevada at 1935 m a.s.l., and the isolated Simeonof Island (SIME), AK, in the Aleutian range. The same decreasing trend in EC/PM ratios with increasing PM_{2.5} mass was noticed at both sites. Conversely, OC/ PM ratios generally increase with PM_{2.5} concentrations ranging from \sim 5 µg/m³ up to \sim 80 µg/m³. This trend indicates that particulate organic matter plays a major role in PM pollution episodes in the western USA. Furthermore, OC/EC ratios steadily increase with PM_{2.5} concentrations ranging from $\sim 1 \, \mu \text{g/m}^3$ to $\sim 80 \, \mu \text{g/m}^3$, consistent with an increased contribution of wildfires and/or an increased fraction of SOA as PM2.5 mass increases. The OC/EC ratio at Simeonof Island, AK, is particularly low compared to other sites.

Clear seasonal variations in the $PM_{2.5}$ carbonaceous content are observed independently of $PM_{2.5}$ levels (Fig. 9). The EC/PM ratio is at its minimum in April to September, and at its maximum in December and January, indicating additional sources of EC during winter, possibly from domestic heating. The seasonal cycle in OC/PM is less pronounced, with a minimum in April, and a maximum in August to November. Consequently, OC/EC ratios follow a marked seasonal pattern, with a minimum in December to March and a maximum in July to September, consistent with increased wildfire activity and photochemical formation of SOA in summer (Watson et al., 2009).

For the other 88 background sites in the remainder of North America, the relationship between EC/PM and PM_{2.5} mass concentrations (Fig. 8, right) is similar to that observed in the western USA. The primary difference lies in the shape of the upper bound (84th percentile), which forms a bell shape for PM_{2.5} concentrations ranging from \sim 8 to 40 μ g/ m³, and peaking around 20 μg/m³. The similarity between this curve and the one representing EC/PM vs. PM_{2.5} mass concentrations at urban sites (Fig. 8, right) suggests that high PM episodes at regional background sites could be due to pollution advection from upwind urban areas, where EC/PM ratios are on average higher. OC/PM ratios are also generally higher at urban sites compared to regional background sites, but the difference is less than for EC/PM ratios. At urban sites, OC/EC ratios are lower and minimally associated with PM2.5 mass concentrations, suggesting that they reflect the chemical composition of the emissions. In contrast, OC/EC ratios increase with PM_{2.5} mass concentrations at the North American regional background sites, similar to what was observed in the western USA, indicating the importance of wildfires and SOA. Compared to the western USA, the seasonal cycles in the carbonaceous content of PM2.5 in the remainder of North America are similar (Fig. 9).

In summary, urban sites in the USA are characterized by higher EC/

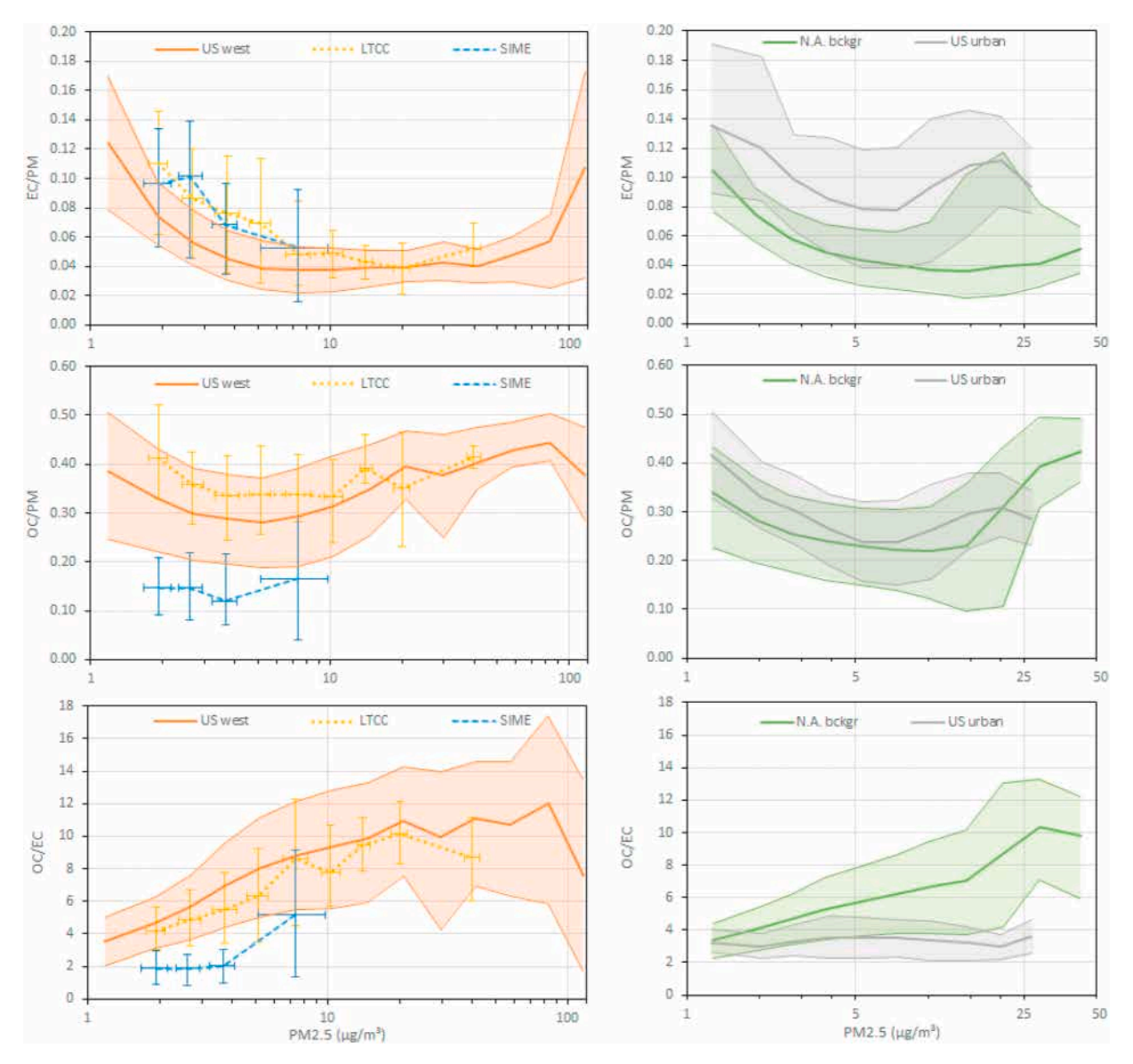


Fig. 8. EC/PM, OC/PM and OC/EC ratios in PM_{2.5} vs PM_{2.5} mass at (left) regional background sites across the western USA, and (right) urban sites (US urban) and regional background (N.A. bckgr) in the remainder of North America.

PM and lower OC/EC ratios compared to regional background sites, reflecting a greater influence of primary emissions at urban sites. The seasonal cycles in EC/PM and OC/EC ratios with maximums in winter and summer, respectively, can be explained by a combination of higher EC emissions in winter related to domestic heating and higher concentrations of OC in summer resulting from enhanced SOA formation and wildfires. Processes that generate OC are primarily responsible for regional $PM_{2.5}$ pollution events in North America.

3.2.3. Comparison between $PM_{2.5}$ and PM_{10} carbonaceous contents in the Andean region of Bolivia

In Chacaltaya (BO), $PM_{2.5}$ OC/EC ratios are not statistically different from those in PM_{10} , except in MAM, where OC/EC ratios are particularly lower in the $PM_{2.5}$ fraction (Fig. S4). This cannot be related to biogenic primary OC, which mainly sits in the in the $PM_{2.5}$ fraction in Chacaltaya (Moreno et al., 2024), but more probably to longer transport times leading to increased loss of coarse particles, including carbonate-rich mineral dust, during this period.

In La Paz (BO), there is no statistically significant dependence of the $PM_{2.5}/PM_{10}$ ratio on PM_{10} mass concentrations for either EC or OC

(Fig. S4). As PM_{10} concentrations greater than 50 $\mu g/m^3$ mainly occurred in the dry season months from May to September, and PM_{10} concentrations less than 30 $\mu g/m^3$ occurred mainly in the wet months January–March (Fig. 6), this suggests that the distribution of EC and OC between PM_{10} and $PM_{2.5}$ does not strongly depend on season either. The amount of EC in $PM_{2.5}$ is on average not statistically different from the amount of EC in PM_{10} , meaning that the amount of EC in the coarse fraction (PM_{10} - $PM_{2.5}$) is not significantly different from zero. In contrast, about 25 % of OC in PM_{10} is found in the coarse fraction, probably due to a significant contribution of carbonate carbon to OC.

3.3. Asia

3.3.1. PM₁₀

 PM_{10} OC and EC data meeting the selection criteria were obtained from five sites in Asia (Table S1). About 30 to 60 data points were available from Bangkok (Bangk), Chiang Mai (Chian), and Songkhla (Songk) in Thailand. Although the data from these distant sites cover different ranges of PM_{10} mass concentrations, EC/PM, OC/PM, and OC/EC are similar in the overlapping range from 65 to 130 μ g/m³ (Fig. S6).

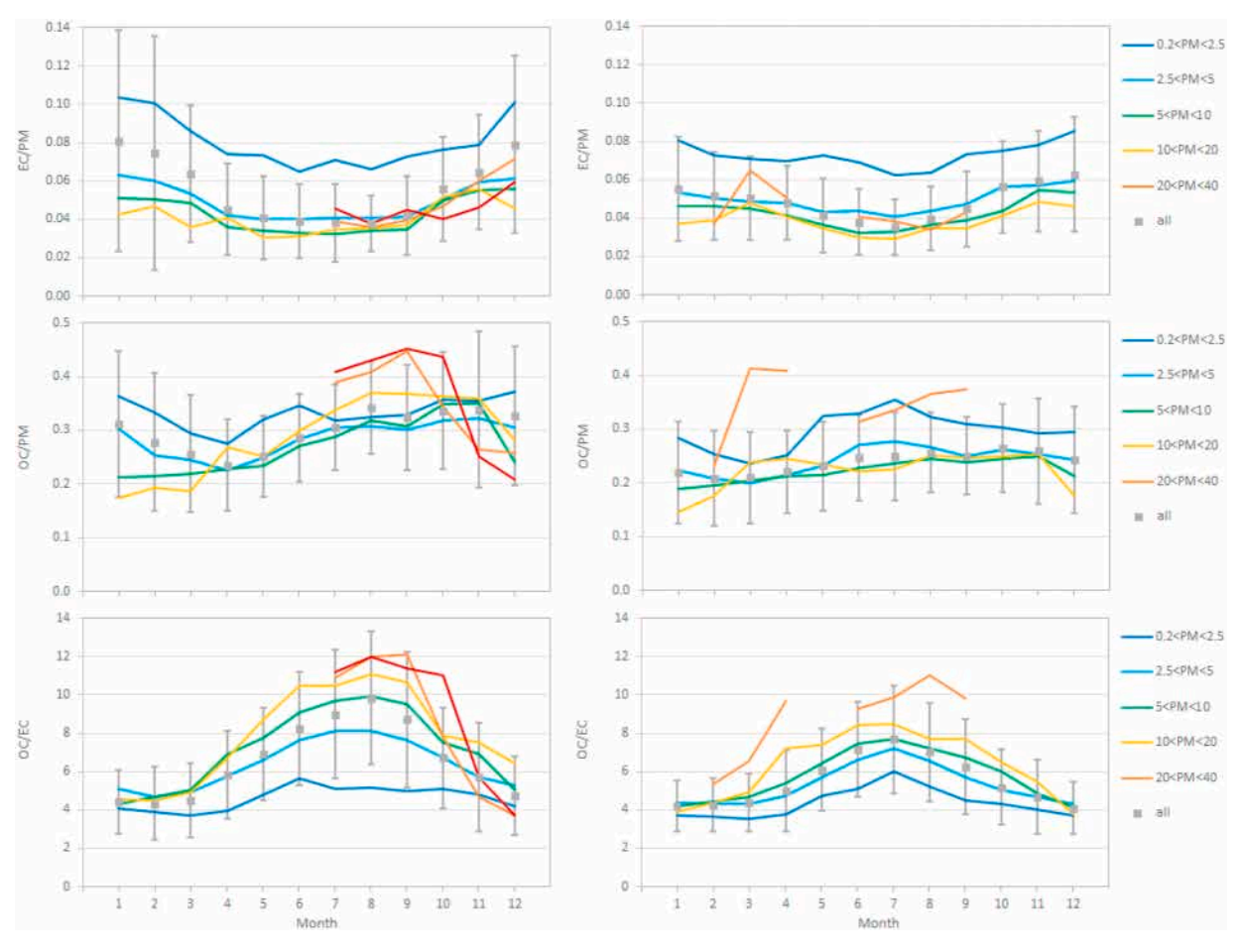


Fig. 9. Seasonal variations in the EC/PM, OC/PM and OC/EC ratios in PM_{2.5} at regional background sites across (left) the western USA and (right) the remainder of North America

Therefore, the data sets from these three sites were merged for producing the curves "Thailand" in Fig. 10. In the Thailand group, EC/PM₁₀ ratios increase with PM₁₀ mass concentrations for PM₁₀ > 80 μ g/m³, indicating that combustion processes are major sources of PM₁₀ during acute particulate air pollution episodes. OC/PM₁₀ ratios also increase with mass concentrations for $PM_{10} > 60 \mu g/m^3$, which again points to carbonaceous aerosol as major contributors to particulate pollution events. Conversely, EC/PM $_{10}$ ratios decrease in Seoul, KR, for PM $_{10}$ mass concentrations increasing from about 10 to 30 µg/m³, and again for PM₁₀ mass concentrations greater than \sim 60 µg/m³. At the background site located in Anmyeon-do Is., KR, EC/PM₁₀ ratios are less dependent on PM_{10} mass concentrations although values observed for $PM_{10} > 80$ $\mu g/m^3$ are on average about half of those for $PM_{10} < 30 \,\mu g/m^3$. OC/PM₁₀ ratios also decrease with PM₁₀ at both sites in Korea (Fig. 10). These observations suggest that carbonaceous aerosol in general, and combustion processes in particular, are not responsible for the high PM₁₀ pollution events in Korea. OC/EC ratios steadily decrease with PM₁₀ mass concentrations in Anmyeon-do, but are quite independent of PM₁₀ levels at Seoul, KR, and in Thailand.

For the Thailand group, both EC/PM and OC/PM ratios are significantly greater during the northern Thailand dry season from December to March and smaller from May to October (Fig. S7), which is consistent with agricultural waste burning being a main source of carbonaceous aerosol in Thailand. However, maximum OC/EC ratios in August to December do not coincide with the biomass burning period. Seasonal variations cannot be clearly described at the two Korean sites but appear to differ from each other, probably due to different sources, processes, and transport patterns occurring across the year at both sites.

Seasonal variations in PM_{10} carbonaceous content are different in

Thailand (7–18°N), where agricultural biomass burning during the dry season plays a major role, compared to Korea (36–38 °N) where multiple factors interact.

3.3.2. PM_{2.5}

 $PM_{2.5}$ OC and EC datasets meeting the selection criteria were collected from 10 sites in China, 14 in India, 103 in Japan, and 3 in Thailand. Due to the much larger number of Japanese sites, data from Japan were analyzed separately (Section 3.3.2.1). Only one site in India had carbonaceous aerosol characteristics similar to those in China and Thailand. Therefore, data from India are also discussed separately (Section 3.3.2.3).

3.3.2.1. Japan. The number of data points per site ranged from 65 to 1213 and averaged 267. The curves representing EC/PM_{2.5} vs. PM_{2.5} mass for each site (Fig. S8) form a dense bundle of lines, at least for PM_{2.5} concentrations greater than $\sim 10 \,\mu\text{g/m}^3$, with a few outliers. Data from the 87 sites with similar EC/PM $_{2.5}$ vs. PM $_{2.5}$ relationships were merged to calculate the mean and percentile values shown in Fig. 11 as the Japanese regional background (Bckgr). At these sites, EC/PM_{2.5} ratio values and variability both steadily decrease as PM2.5 mass concentrations increase from ~ 2 to $\sim 50 \,\mu\text{g/m}^3$. Seven sites with higher EC/PM_{2.5} ratios - Chiba, Hayashima (Hayas), Kunitashi (Kunit), Kyoto, Okaza and Sapporo (Sappo) - constitute the "urban" group, where EC/PM_{2.5} ratios also generally decrease with rising PM_{2.5} concentrations. Low EC/PM_{2.5} ratios were observed at Aomori (Aomor), Hamada (Hamad), Kirishima (Kiris), Kunigami (Kunig), Noto supersite (NotoG), Ogasawara (Ogasa), Okinishima (Okini), and Tottori (Totto), all located on the sea shore or on small islands. For these eight marine sites, EC/PM2.5 ratios remain

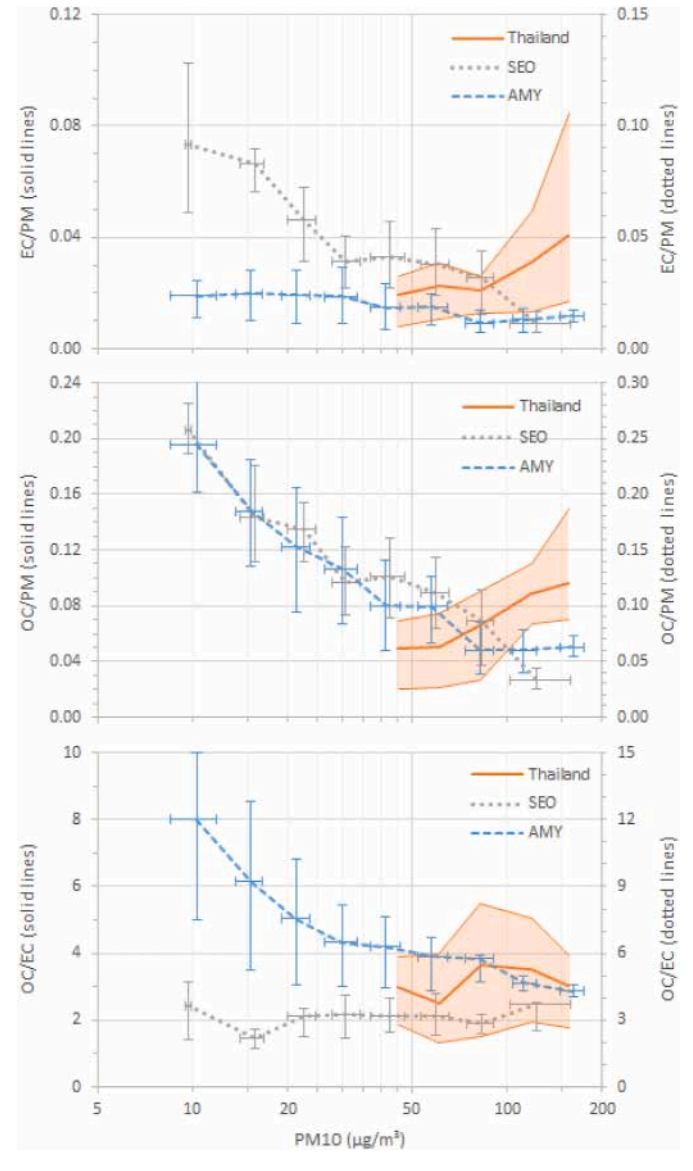


Fig. 10. EC/PM, OC/PM and OC/EC in PM_{10} vs PM_{10} mass at 3 locations in Asia. Measurements were performed with different thermal protocols in Thailand and Korea, and cannot be directly compared.

quite independent from PM mass concentrations for PM $_{2.5}$ ranging from ~ 8 to 40 $\mu g/m^3$, potentially representing the regional marine background.

OC/PM_{2.5} ratios also mostly decrease with increasing PM_{2.5} mass, and the OC/PM_{2.5} gradient from marine to urban sites is similar to that of EC/PM_{2.5}, albeit less pronounced. The variability in OC/EC ratios is even less, both across the 3 site groups and in relation to PM_{2.5} mass concentrations. However, OC/EC ratios consistently increase from urban to regional background to marine sites for PM_{2.5} $> 10~\mu g/m^3$, suggesting a larger contribution of SOA when moving away from cities.

Fig. 12 shows that the decrease in EC/PM_{2.5} ratios as a function of PM_{2.5} appears for each season, and that the seasonal cycle in EC/PM_{2.5} ratios, with a maximum during autumn and winter and a minimum during the spring and summer, occurs across all PM_{2.5} mass concentration ranges. Such seasonal variations likely reflect increased emissions of EC during autumn and winter, most probably associated with domestic heating, as well as manufacturing industries and construction activities (EDGAR, 2024). In contrast, OC/PM ratios do not exhibit any consistent seasonal cycles, resulting in OC/EC ratios showing seasonal variations that are inverse to those of EC/PM. Such variations may be attributed to

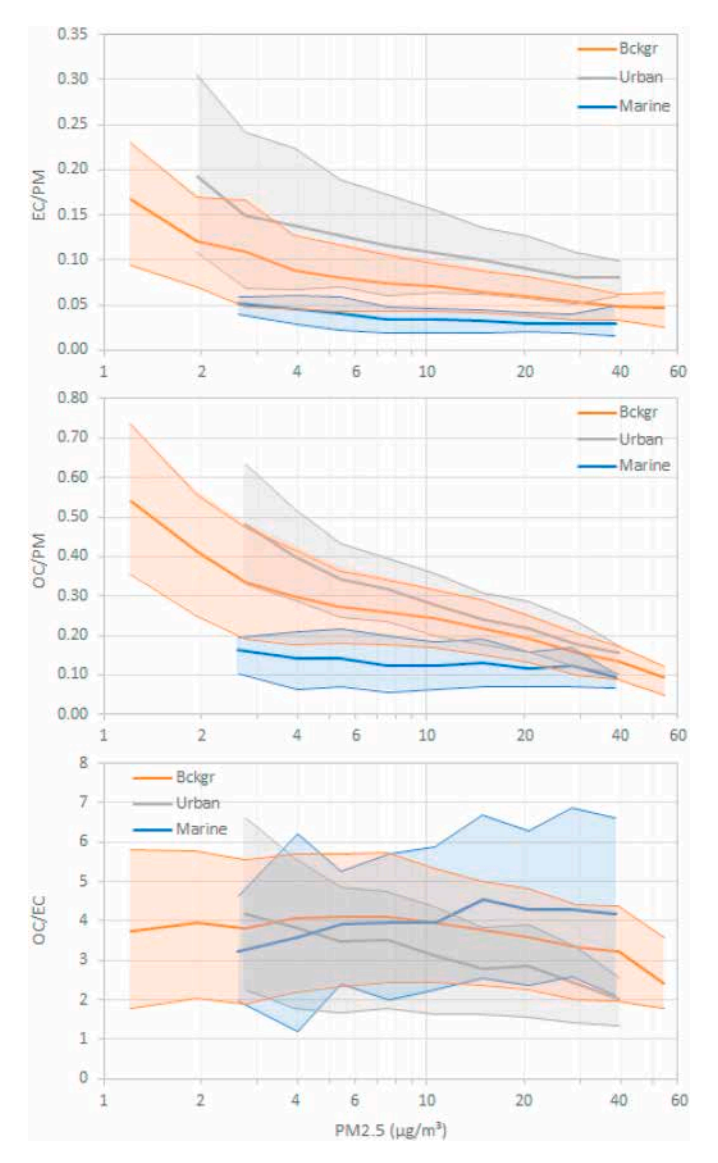


Fig. 11. EC/PM, OC/PM and OC/EC ratios in $PM_{2.5}$ vs $PM_{2.5}$ mass at marine, urban, and regional background sites in Japan.

the increased photochemical production of SOA in spring and summer. Similar seasonal variations are observed at urban and marine sites (Fig. S9).

3.3.2.2. China, Korea, and Thailand. $PM_{2.5}$ EC/PM, OC/PM, and OC/EC ratios as a function of $PM_{2.5}$ mass for each site are shown in Fig. S10. Data from Indonesia are not further discussed due to their limited time coverage. Fig. S10 shows similar EC/PM vs. PM, OC/PM vs. PM, and OC/EC vs. PM relationships for eleven sites (nine in China and two in Thailand), and highlights Bangkok (Bangk) in Thailand as an outlier with outstanding OC/EC ratios. Therefore, data from Bangkok were plotted independently, as well as data from Bangyeong Island (ByIs) in Korea, due to a different $PM_{2.5}$ mass concentration range (Fig. 13).

Data from the ensemble of eleven Asian sites (CN + TH) cover PM_{2.5} mass ranging from $\sim\!20$ to 300 $\mu g/m^3$. Within this range, EC/PM ratios do not strongly depend on PM_{2.5} mass concentrations (Fig. 13). In contrast, a steady decrease in EC/PM ratios for PM_{2.5} mass concentrations increasing from $\sim\!5$ to $\sim\!60~\mu g/m^3$ is observed at Baengnyeong Island, KR. Similar observations can be made about OC/PM_{2.5} ratios. OC/EC is quite independent of PM_{2.5} mass at CN + TH sites, but increases with PM_{2.5} from $\sim\!30~\mu g/m^3$ and $\sim\!45~\mu g/m^3$ at Baengnyeong Island, KR, and Bangkok, TH, respectively. This trend is consistent with

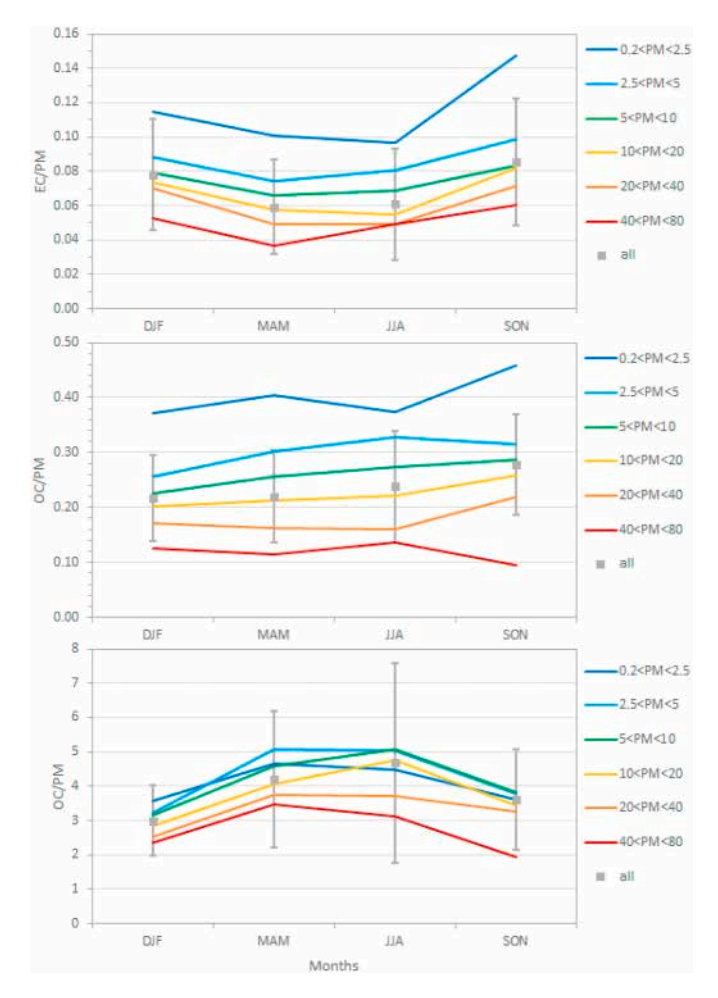


Fig. 12. Seasonal variations in the EC/PM, OC/PM and OC/EC ratios in $PM_{2.5}$ across 92 regional background sites in Japan.

the features observed in PM_{10} at Anmyeon-do Is. (KR) and in Thailand within the overlapping mass concentration range.

Seasonal variations in PM_{2.5} in Thailand are also consistent with those observed in PM₁₀ (Fig. S7). For the nine sites in northeastern China, there is a large variability in EC/PM and OC/PM across the various PM_{2.5} ranges in JJA, during the warm and wet season (Fig. 14). Significantly higher EC/PM and OC/PM ratios are observed in DJF and SON. Increased emissions from open biomass burning in Northeast China from February to May and September to November were reported by Shi et al. (2021) and Huang et al. (2024), while increased emissions from fossil fuel and biomass burning combustion for domestic heating are reported to peak in DJF (EDGAR, 2024). There are no statistically significant seasonal variations in the OC/EC ratio, suggesting a constant predominance of primary carbonaceous aerosol in northeastern China. In both Baengnyeong Island, KR, and Bangkok, TH, a consistent minimum in OC/PM and OC/EC for all PM2.5 concentration ranges is observed in JJA during the wet season (Fig. S11), probably for different reasons (see 3.3.1). During the summer monsoon, air circulation patterns prevent westward pollution transport to Baengnyeong Island (Lee et al., 2015), and low OC concentrations in Bangkok were attributed to negligible biomass burning emissions (Sahu et al., 2011).

3.3.2.3. India. Among the 14 Indian sites (Table S1), Mohali (Moha) and Srinagar (Srin) exhibit high EC/PM and OC/PM ratios, at least within specific ranges of PM_{2.5} (Fig. S12). Data from these two sites, along with data from Darjeeling (Darj) and Delhi, obtained with a different thermal protocol, are plotted independently (Fig. 15). High and highly variable OC/EC ratios are observed in Bhopal (Bhop) and Mysuru

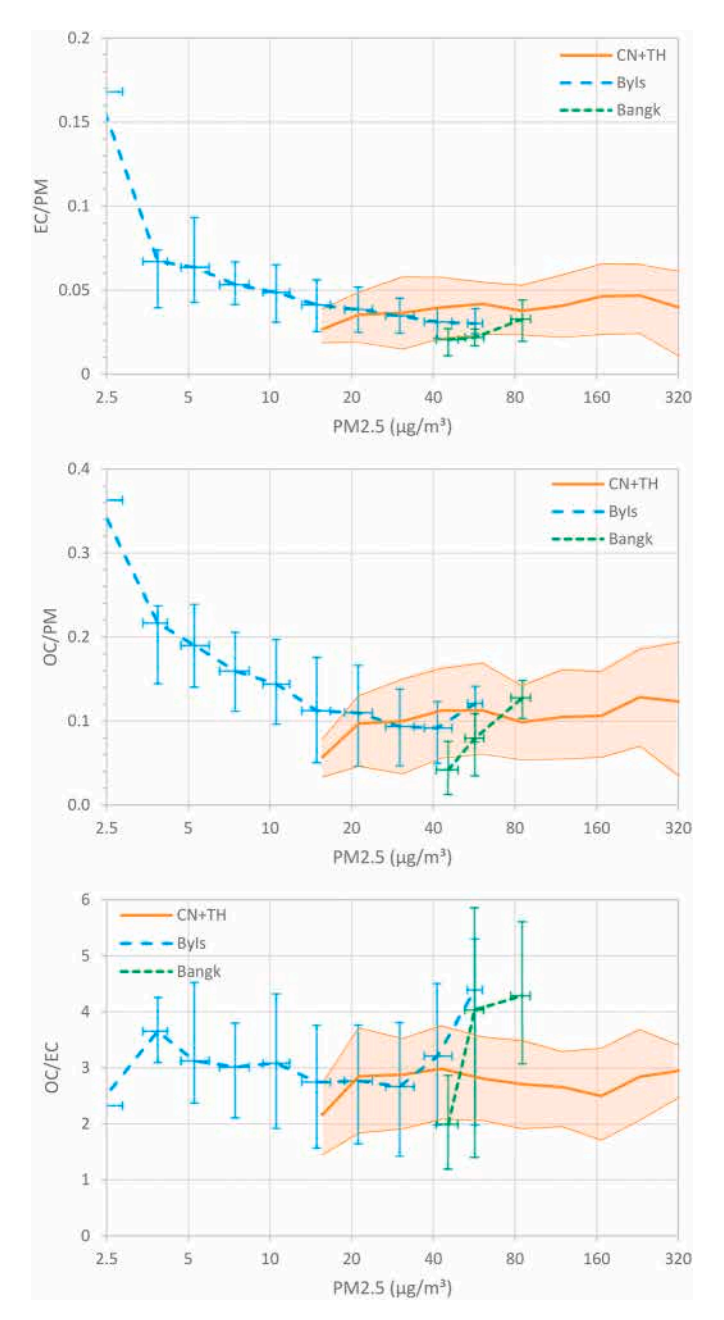


Fig. 13. EC/PM, OC/PM and OC/EC ratios in ${\rm PM}_{2.5}$ vs ${\rm PM}_{2.5}$ mass in China, Korea and Thailand.

(Mysu). Due to differences between these two sites in terms of geography, potential sources for OC and EC, and observed PM_{2.5} concentration ranges, they are also examined independently, although EC/PM and OC/ PM ratios are quite similar in the overlapping $PM_{2.5}$ range, i.e. $10\text{--}60\,\mu\text{g}/$ m³ (Fig. 15). Across the remaining eight Indian sites, EC/PM and OC/PM ratios are less variable, and these data were averaged as India-1. For this group, the mean EC/PM ratio increases with PM25 mass in range 12–120 μg/m³ (Fig. 15). This contrasts with Darjeeling (Darj) and Mohali (Moha) where EC/PM decreases with increasing PM_{2.5} mass. At Bhopal and Mysuru, EC/PM ratios also slightly increase with PM_{2.5} mass in the range 22-60 µg/m³, but EC/PM are on average half of those of India-1. In Delhi, there is no consistent trend in EC/PM as a function of PM_{2.5} concentrations. For the India-1 group, the mean OC/PM ratio is at its minimum for PM_{2.5} mass between 15 and 40 μ g/m³ and increases by up to 60 % for larger PM_{2.5} concentrations. Such a trend is not observed at other sites in India (Fig. 15), where the absence of strong and

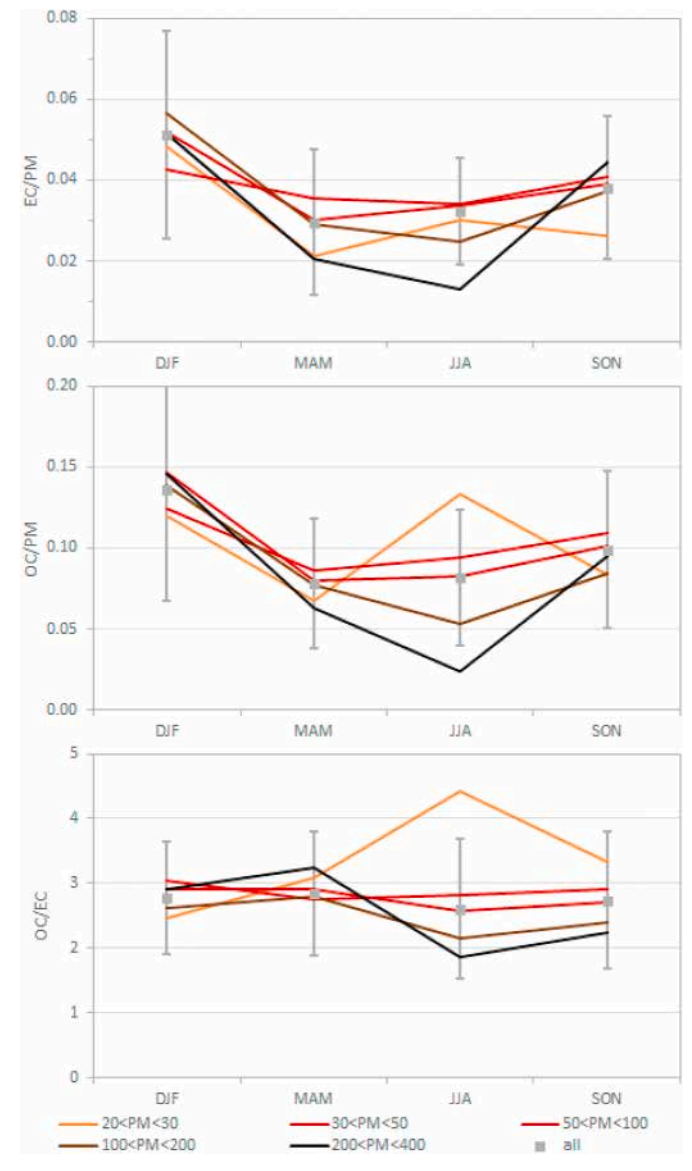


Fig. 14. Seasonal variations in the EC/PM, OC/PM and OC/EC ratios in $PM_{2.5}$ for the ensemble of 11 sites located in China and Thailand.

consistent dependence of EC/PM and OC/PM ratios on $PM_{2.5}$ mass suggests that particulate pollution episodes are not primarily due to increased emissions of carbonaceous species, but rather to, e.g., weakened pollution dilution or removal processes under specific meteorological situations. Mean OC/EC ratios are even less dependent on $PM_{2.5}$ and vary within a factor of two for each site or group of sites (India-1), except at Bhopal and Mysuru, where OC/EC ratios are large and highly variable over a wide range of $PM_{2.5}$ concentrations, suggesting a larger variety in carbonaceous aerosol sources at these two sites.

Seasonal variations in EC/PM and OC/PM ratios are observed in the ensemble of sites in India-1 for PM $_{2.5}$ mass >20 µg/m 3 (Fig. 16). Minima are observed from June to September, corresponding to India's typical wet summer monsoon season (Pai et al., 2020), which could be related to limited agricultural biomass burning. Similar seasonal cycles are observed at Bhopal, Mysuru and Delhi, with minima shifted by 1–3 months though (Fig. S13). At Darjeeling, both EC/PM and OC/PM ratios are maximal in June–November (Fig. S13), due to air mass transport from the more polluted Indo-Gangetic Plain during the summer monsoon season, and from the Tibetan plateau where forest fires occur in winter. At Mohali and Srinagar (Fig. S13), seasonal variations in EC/PM and OC/PM are complex, suggesting variable impacts of

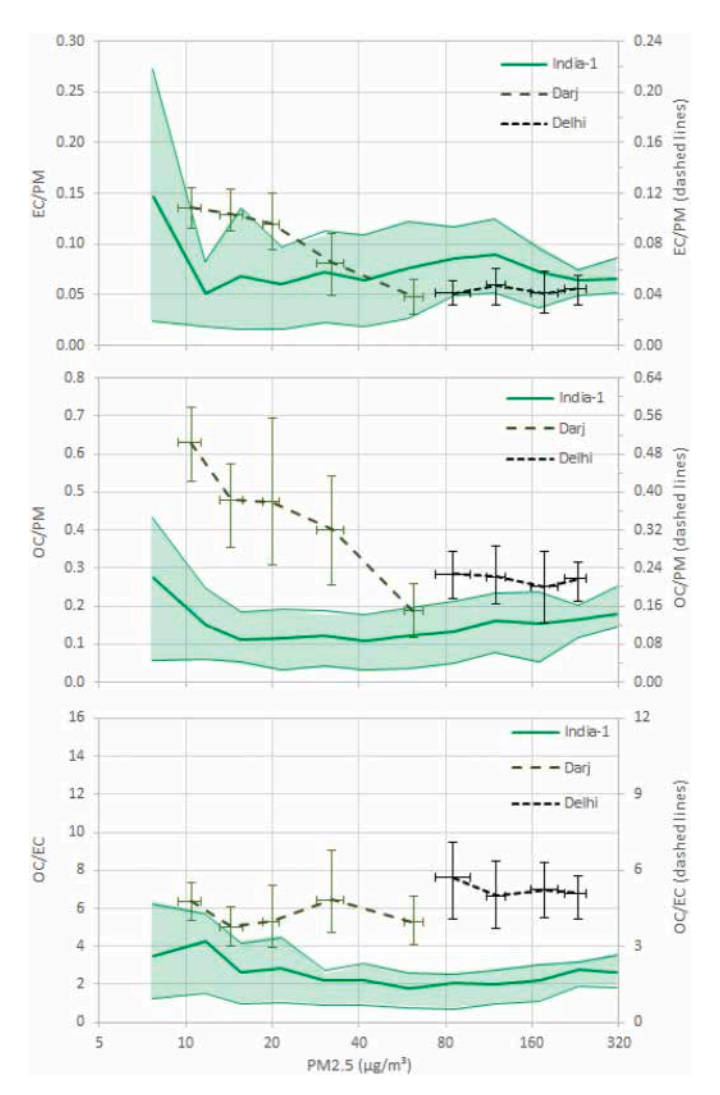


Fig. 15. EC/PM, OC/PM and OC/EC ratios in $PM_{2.5}$ vs $PM_{2.5}$ mass in India. India-1 represents a set of 8 sites in India. Data from Darjeeling (Darj) and Delhi were obtained with a different thermal protocol and cannot be directly compared with others.

different sources and processes across the year. There are no clear seasonal variations in the OC/EC ratios at any site or site group in India, except in Mohali, where OC/EC ratios reach a maximum in October–January (Fig. S12), i.e. the dry seasons during which agricultural residue burning was identified as the dominant aerosol source (Venkataraman et al., 2024).

In brief, the variations in $PM_{2.5}$ OC and EC contents in India are primarily influenced by the monsoon cycle, which governs pollution transport patterns, aerosol wet deposition, and open biomass burning intensity. Consequently, elevated EC/PM and OC/PM ratios are observed from November to February, i.e. the dry season in large parts of India, during which the highest PM_{10} levels are recorded. However, OC/EC ratios remain low quite independently from seasons and $PM_{2.5}$ concentrations, indicating a limited contribution of SOA to OC, at least at the sites within the India-1 group. Due to India's vast geographic size and environmental diversity, particular features in $PM_{2.5}$ carbonaceous content are observed at several specific sites.

3.4. Europe

3.4.1. PM₁₀

For the PM₁₀ size fraction, EC and OC data meeting the selection

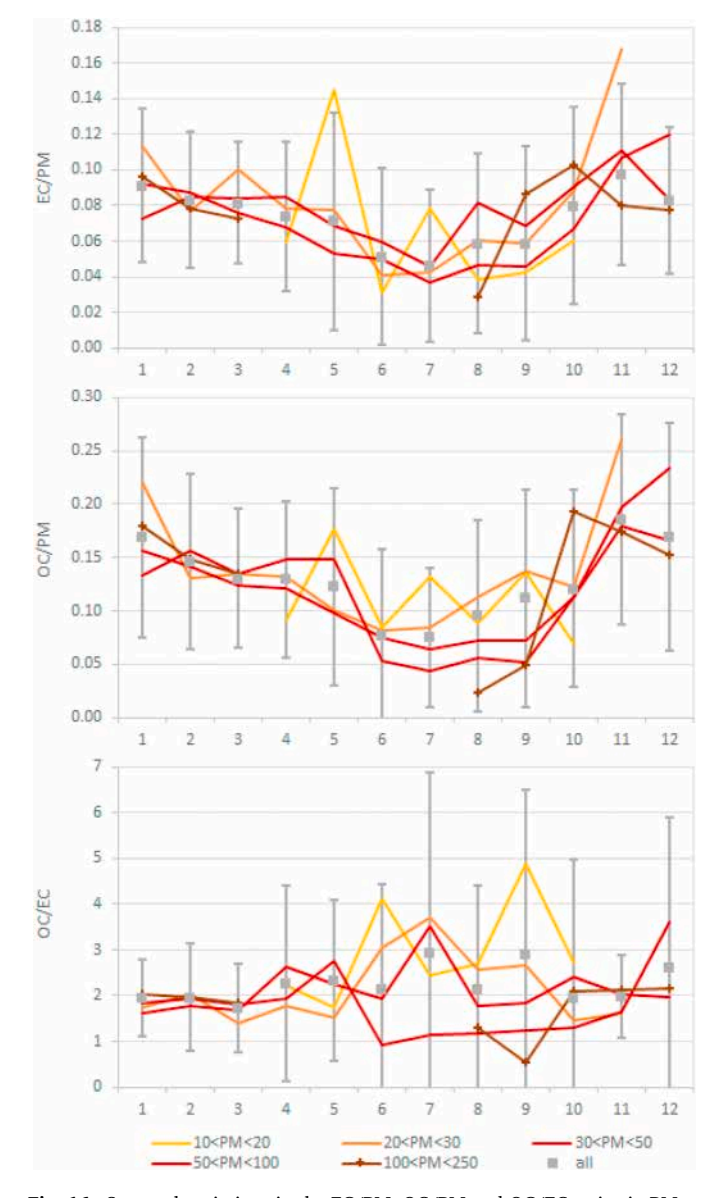


Fig. 16. Seasonal variations in the EC/PM, OC/PM and OC/EC ratios in $PM_{2.5}$ for the ensemble of 8 sites (India-1) located in India.

criteria were retrieved for ten sites across Europe. Plotting EC/PM and OC/PM ratios as a function of PM₁₀ mass concentrations reveals similarities in PM₁₀ carbonaceous content across Europe, with three outliers: Cabauw (CBW), NL, and Melpitz (MEL), DE, with higher EC contents, and Agia Marina (CYP), CY, with lower OC contents (Fig. S14). Data from the seven other sites were grouped to form the main "Europe" group (Fig. 17). For these sites, EC/PM ratios decrease with PM₁₀ mass increasing from ${\sim}2$ to ${\sim}40~\mu\text{g/m}^3,$ and the range of EC/PM ratios for a given PM₁₀ concentration is quite narrow, the 86th percentile being less than twice the 14th percentile. A similar decrease is observed at CBW, NL, and CYP, CY, but not at MEL, DE, where EC/PM ratios increase by about 35 % as PM_{10} mass quadruples from 20 $\mu g/m^3$ to 80 $\mu g/m^3$. Together with the increase of OC/PM ratios with PM₁₀ mass concentrations, this suggests that uncontrolled combustion sources largely contribute to the highest PM₁₀ concentrations at MEL, which is not the case at the other sites. For the main group of seven European sites (Europe), the OC/EC ratio increases with PM₁₀ mass (Fig. 17), although this trend is not consistent across all seven sites (Fig. S14).

The significant minimum in EC/PM and the maximum in OC/EC observed in JJA probably results from reduced EC emissions from

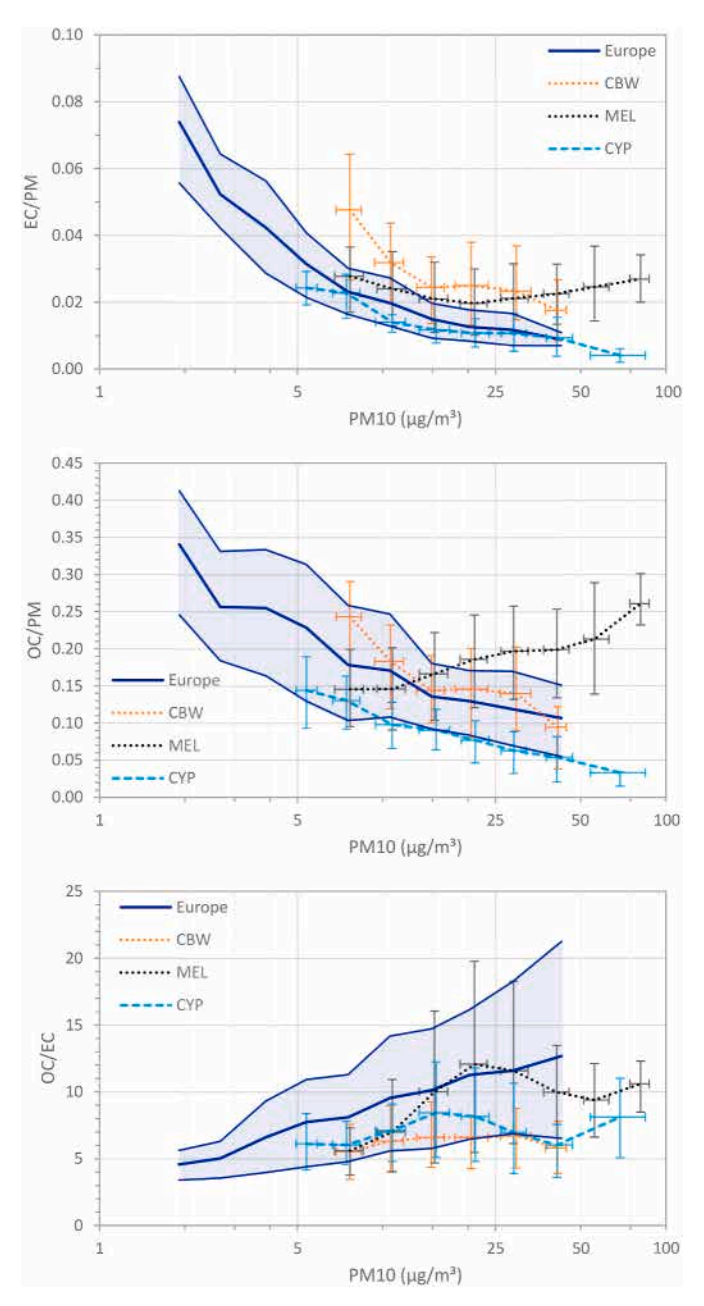


Fig. 17. EC/PM, OC/PM and OC/EC in PM_{10} vs PM_{10} mass across regional background sites in Europe.

domestic heating and enhanced SOA production in summer. The absence of significant seasonal variations in OC/PM ratios for the "Europe" group (Fig. 18) suggests that nearly equally efficient OC production processes take place throughout the year, like e.g. amplified condensation of semi-volatile organic species in winter, and enhanced photochemical formation of SOA in summer.

3.4.2. PM_{2.5}

For the $PM_{2.5}$ size fraction, EC and OC data from 22 sites across Europe were selected. The set of curves representing EC/ $PM_{2.5}$ vs. $PM_{2.5}$ mass (Fig. S15) can be divided into two groups: Europe-1, consisting of 15 consistent curves, mainly from western and northern Europe sites, and Europe-2, comprising seven curves, mainly from central and eastern Europe sites.

For both groups, EC/PM ratios decrease as PM_{2.5} mass increases from ~ 1 to $\sim 15~\mu g/m^3$, and level off for Europe-1 or slightly increase for

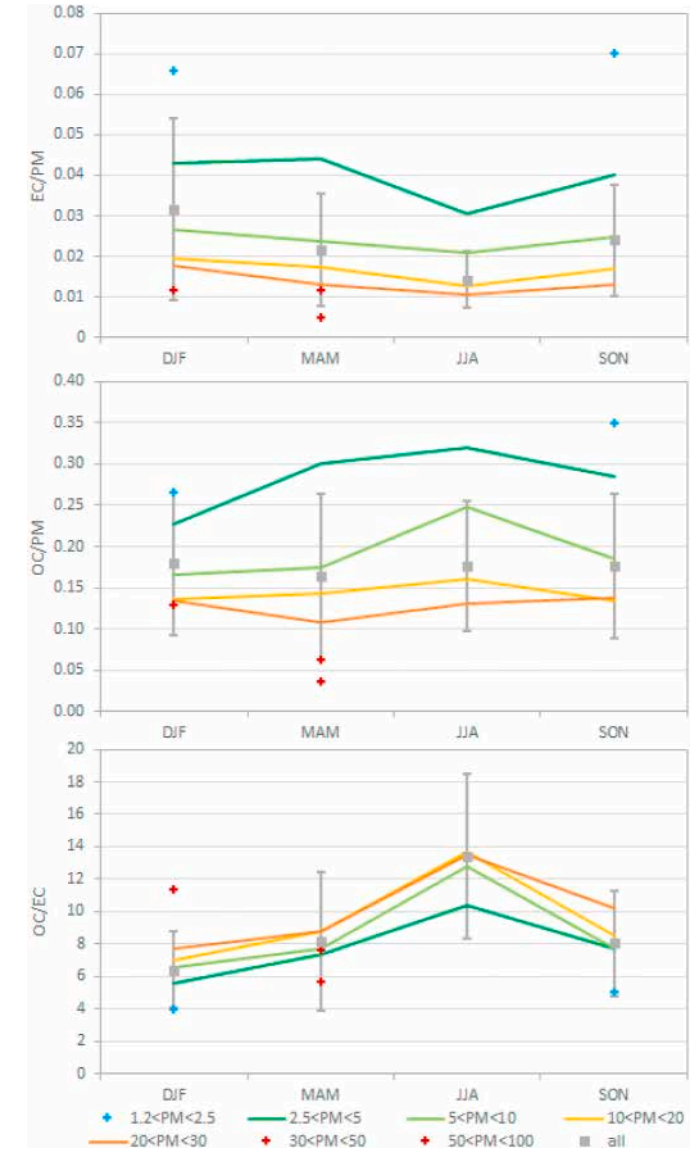


Fig. 18. Seasonal variations in EC/PM, OC/PM, OC/EC ratios in PM_{10} in the "Europe" group of 7 sites.

Europe-2 as PM_{2.5} mass increases from ~ 15 to $\sim 50~\mu g/m^3$ (Fig. 19). This suggests that particulate air pollution episodes are not particularly due to increased contributions of emissions from combustion processes. Similar shapes are observed for the OC/PM_{2.5} vs PM_{2.5} curves for both groups. The flattening of the EC/PM_{2.5} vs. PM_{2.5} and OC/PM_{2.5} vs. PM_{2.5} curves for PM_{2.5} mass concentrations exceeding $\sim 10~\mu g/m^3$ indicates that PM pollution events are mostly due to a reduction in atmospheric dispersion controlled by local meteorological conditions, rather than by increases in specific sources. This is confirmed by the weak dependence of OC/EC on PM mass for PM_{2.5} > 6 $\mu g/m^3$.

The mean seasonal variations for Europe-1 and Europe-2 (Fig. 20) resemble those for the previous group of sites with PM_{10} data. For all $PM_{2.5}$ levels, EC/PM ratios are at a minimum in JJA, while OC/PM ratios show less variability, resulting in maximum OC/EC ratios in JJA. The increase in OC/EC ratios during summer, along with the increase in OC/EC ratios with $PM_{2.5}$ mass during this season, highlight the importance of SOA. The fact that OC/PM still decreases with increasing $PM_{2.5}$ mass in JJA suggests that something increases more than secondary organic carbon during photochemical PM pollution episodes, possibly the oxidation state of OC and more probably the amount of secondary inorganic aerosol (SIA). Similar negative gradients in EC/PM, OC/PM,

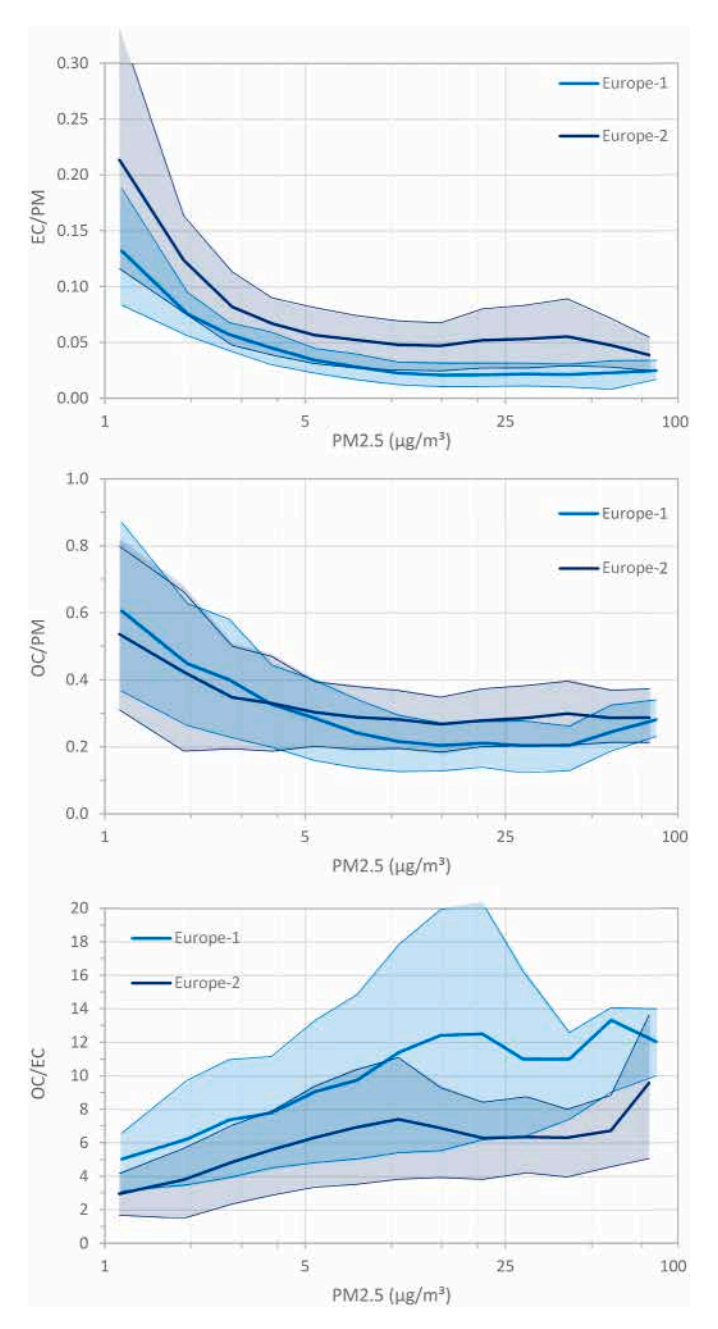


Fig. 19. EC/PM, OC/PM and OC/EC ratios in PM_{2.5} vs PM_{2.5} mass in western and northern Europe (Europe-1) and central and eastern Europe (Europe-2).

and OC/EC as a function of $\rm PM_{2.5}$ mass are observed during cold months, indicating a major role of SIA formation in PM pollution episodes in winter.

3.4.3. $PM_{2.5}/PM_{10}$ ratios

Simultaneous OC and EC data in PM_{10} and $PM_{2.5}$ were collected from four sites across Europe: BIR and HRD (NO), MEL (DE), and MSY (ES). For EC, the mean $PM_{2.5}/PM_{10}$ ratios ranged from 0.88 to 0.97 and were statistically different from 1 at the of 99.9 % confidence level at MEL and MSY, suggesting the presence of EC in the coarse aerosol fraction ($PM_{10}-PM_{2.5}$). Slight differences between samplers could affect this ratio, whereas a contribution of carbonate carbon evolving as EC during the analysis is less probable. In contrast to EC, the mean $PM_{2.5}/PM_{10}$ ratios for OC, ranging from 0.77 to 0.94 were significantly different from 1 at the 99.9 % confidence level at all sites, indicating the existence of coarse OC sources, particularly at BIR and HRD.

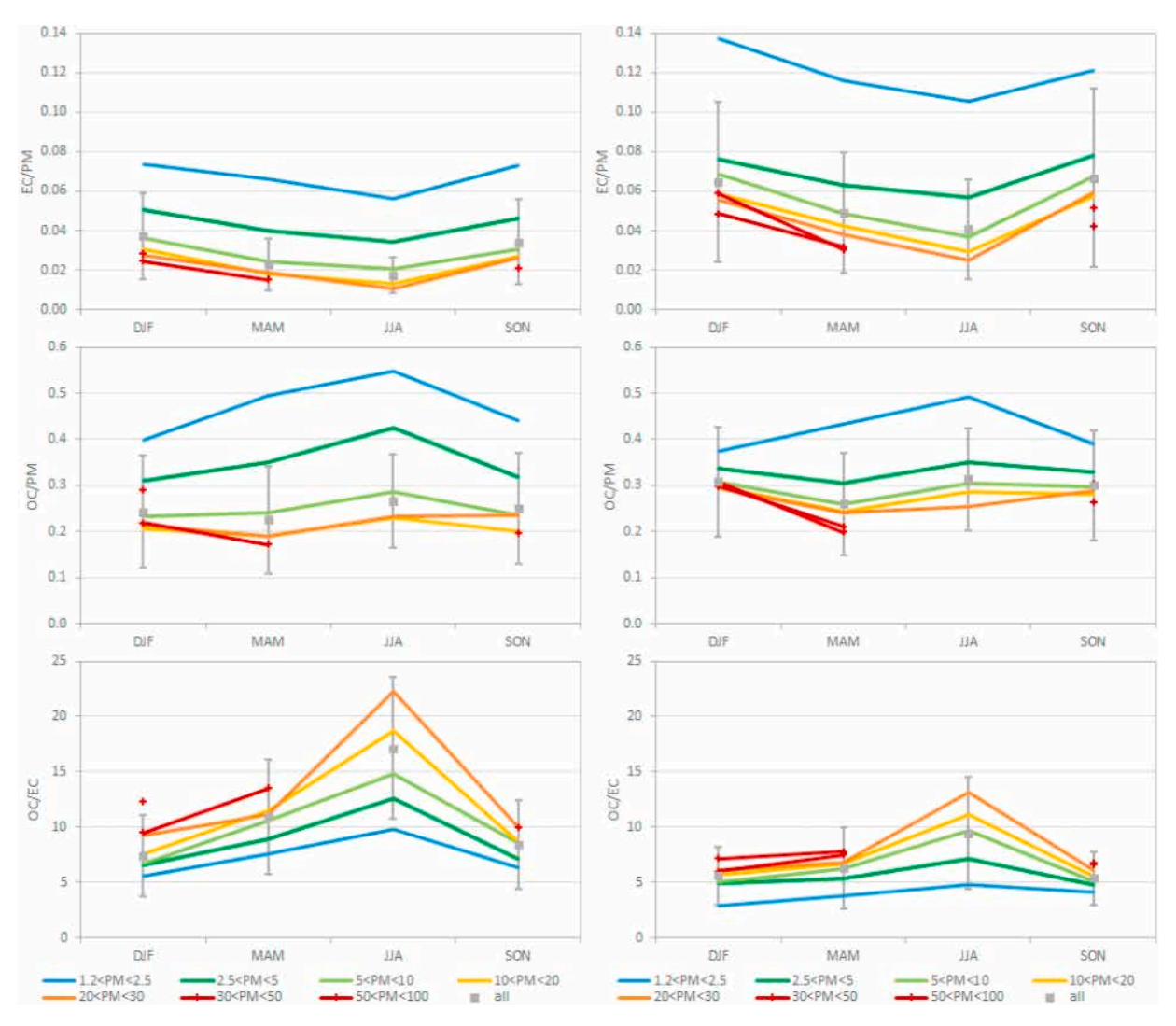


Fig. 20. Seasonal variations in EC/PM, OC/PM and OC/EC ratios in PM_{2.5} in (left) western and northern Europe (Europe-1), and (right) central and eastern Europe (Europe-2).

No strong dependence of $PM_{2.5}/PM_{10}$ with PM mass is observed for either EC or OC (Fig. 21). However, significant seasonal cycles emerge for both EC and OC in MEL, with minimal $PM_{2.5}/PM_{10}$ ratios in JJA for both components, and for OC at both sites in Norway with minimal $PM_{2.5}/PM_{10}$ ratios in JJA and SON (Fig. 22). The latter suggests an increase in the production of coarse OC during these periods. (Yttri, 2011) have previously reported about an increased fraction of coarse OC from biogenic origin in Norway during summer.

In short, PM carbonaceous content in Europe primarily results from the season cycle characteristic of temperate climates. Winter favors the condensation of semi-volatile organics and inorganics (e.g. NH₄NO₃), resulting in lower EC/PM and higher OC/EC ratios during pollution events, but generally not in higher OC/PM ratios. Conversely, summer boosts the production of SOA and SIA (e.g. (NH₄)₂SO₄), leading to reduced EC/PM ratios and elevated OC/EC ratios.

3.5. Worldwide perspective

As noted, OC and EC measurements by thermal-optical analyses have used different methods across the world (Table S1). In the USA and most of Asia, the IMPROVE_A thermal protocol with charring correction is based on sample light reflectance (Chow et al., 2007), although a transmittance pyrolysis correction is also reported by this method. Across Europe and at various sites in Africa, South America, and one in

Asia, the EUSAAR_2 thermal protocol (Cavalli et al., 2010) with charring correction based on sample light transmittance has been used for the past 15 years. In this section, OC and EC data were harmonized as specified below using the conversion factors listed in Table 1 to enable comparisons. The differences and similarities in PM carbonaceous content described below are all robust and unaffected by the harmonization applied.

3.5.1. PM_{2.5} carbonaceous content

In Fig. 23, OC and EC data from Europe, obtained using the EUSAAR_2/T method, have been converted to "IMPROVE_A/R equivalent" data.

The curves depicting EC/PM $_{2.5}$ ratios vs. PM $_{2.5}$ mass form a cluster whose lower and upper boundaries approximately coincide with the curves corresponding to the Japanese marine and urban sites, respectively (Fig. 23). This suggests that there is likely no greater variability in EC/PM $_{2.5}$ worldwide than in a single country like Japan. At regional background sites in North America (N.A. bckgr and US west), in China and Thailand (CH + TH), and western/northern Europe (Europe-1), EC/PM $_{2.5}$ ratios are generally close to the lower values observed at Japanese marine sites. Notably, even lower EC/PM $_{2.5}$ ratios occur at the Virgin Islands in the Caribbean (Fig. 7). In contrast, at urban sites in Bolivia (Bolivia-U), the USA (US urban), and in central and eastern Europe (Europe-2), EC/PM ratios can be as high as those at Japanese urban sites.

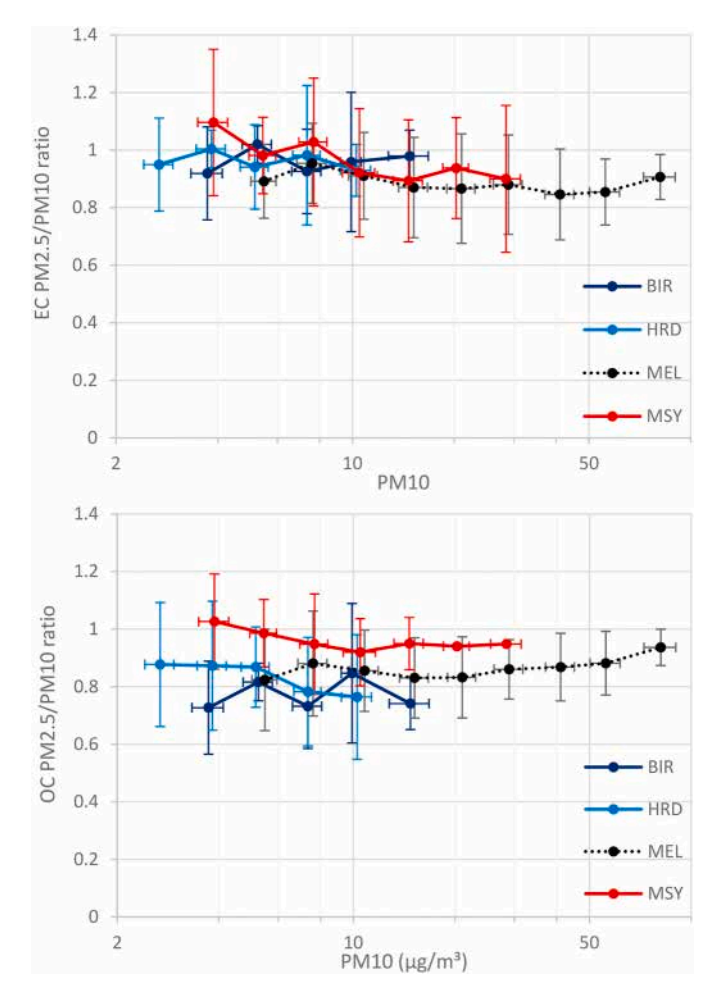


Fig. 21. $PM_{2.5}/PM_{10}$ ratios for EC and OC as a function of PM_{10} mass at 4 sites in Europe.

Over the common $PM_{2.5}$ range of 20–40 $\mu g/m^3$ (Table 3), the mean EC/PM ratio is ~ 0.03 at marine sites in Japan and regional background sites in western and northern Europe, ~ 0.04 in China, Thailand and at regional background sites in North America, ~ 0.06 –0.07 at regional background sites in Japan, central and eastern Europe, and in most of India, and in the range 0.08–0.11 at urban sites in Bolivia, Japan, and North America (Table 3). The increase in EC/PM_{2.5} ratios as PM_{2.5} mass approach their lower values is observed across most site groups, except for China and Thailand that experienced no PM_{2.5} daily concentrations below $20~\mu g/m^3$.

The relationships between OC/PM_{2.5} ratios and PM_{2.5} mass exhibit a wider diversity across the main 11 site groups (Fig. 23). OC/PM ratios are lowest in China, Thailand, India, and at Japanese marine sites, with even lower values observed at Baengnyeong Is., KR, and Bangkok, TH (Fig. 13). Conversely, the highest OC/PM_{2.5} ratios for PM_{2.5} $> 20~\mu g/m^3$ are found in North America, and particularly in the western USA. For PM_{2.5} concentrations ranging from 20 to 40 $\mu g/m^3$, mean OC/PM ratios are between 0.10 and 0.12 in China and Thailand, the group of sites in India-1, and marine sites in Japan, about 0.14 at urban sites in Bolivia, between 0.17 and 0.20 at other site types in Japan and western and northern Europe, about 0.25 in central and eastern Europe, and in the range of 0.31–0.39 in North America (Table 3). For PM_{2.5} $< 8~\mu g/m^3$, OC/PM_{2.5} ratios get similar among North America, Europe, and regional background sites in Japan, following a consistent increasing trend with decreasing PM_{2.5} mass.

The curves representing OC/EC ratios vs. $PM_{2.5}$ mass can be categorized into two groups. At regional background sites in North America (N.A. bckgr, US west), and western and northern Europe sites (Europe-

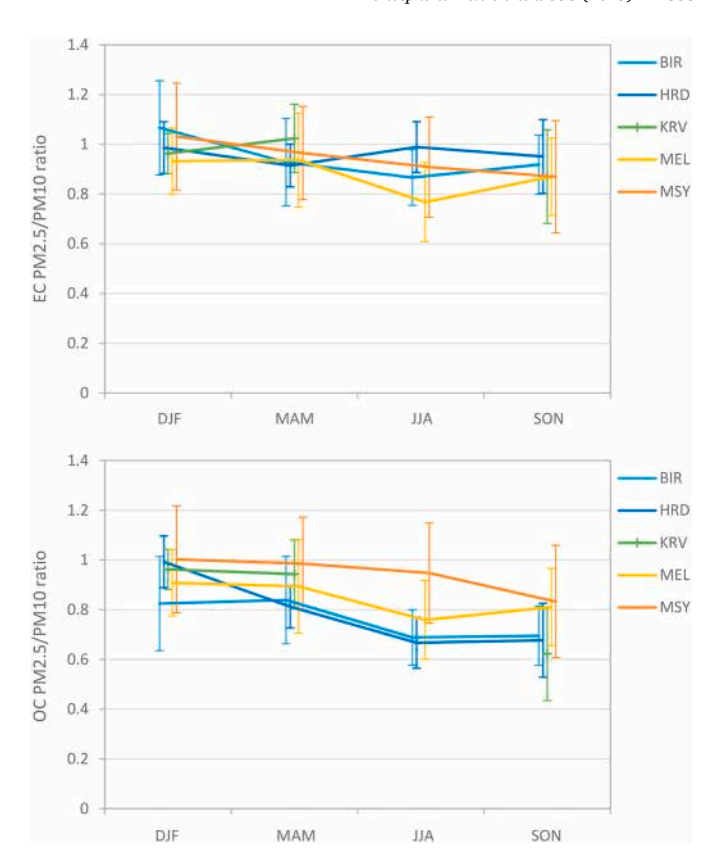


Fig. 22. Seasonal variations in the contribution of $PM_{2.5}$ to PM_{10} for EC and OC at 5 sites across Europe.

1), OC/EC ratios increase by factors of $\sim\!\!3\text{--}4$ as $PM_{2.5}$ mass increases from 1 to 40–120 $\mu g/m^3$. Particularly elevated mean OC/EC ratios ranging from $\sim\!\!8$ to $\sim\!\!10$ in the $PM_{2.5}$ range of 20–40 $\mu g/m^3$ are observed in these regions (Table 3). High OC/EC ratios are also observed at specific sites in India, such as Darjeeling and Delhi (Table 3), Bhopal and Mysuru (Fig. 15), and at Virgin Is. (Caribbean) at low $PM_{2.5}$ concentrations (Fig. 7). For all other site groups, OC/EC ratios are weakly or inconsistently depending on $PM_{2.5}$, and generally remain two to four times lower compared to North America and northwestern Europe across a wide range of $PM_{2.5}$ concentrations (Fig. 23). OC/EC ratios are lower at urban sites compared to background sites within the same region, in line with the observations of Querol et al. (2013) based on measurements in Spain.

3.5.2. PM_{10} carbonaceous content

 PM_{10} samples with mass and carbon values were not available from regions like North America, China, and India. As most of the OC and EC data in the PM_{10} size fraction were produced using the EUSAAR_2/T thermal-optical method, data obtained with the IMPROVE_A/R method at three sites in Thailand and Welgegund in South Africa, and with the NIOSH/T method at two sites in South Korea, were converted to "EUSAAR_2 equivalent" data using the factors listed in Table 1. Therefore, the values for the PM_{10} size fraction shown in Fig. 24 are not directly comparable with those for the $PM_{2.5}$ size fraction shown in Fig. 23, which anyway represent a different set of sites. For direct comparisons, see Tables 3 and 4.

EC/PM₁₀ ratios are higher at urban sites in Bolivia (about 0.05 for PM₁₀ ranging from 30 to 50 μg/m³) compared to other site groups (Fig. 24), and even higher at Bogotá, CO, also in Latin America (Fig. 5). Within "Europe", EC/PM₁₀ ratios are approximately five times lower (e. g., 0.01 within the 30–50 μg/m³ PM₁₀ range), probably because the "Europe" group includes mostly regional background sites. Even at European sites with particularly elevated EC/PM₁₀ ratios such as Melpitz,

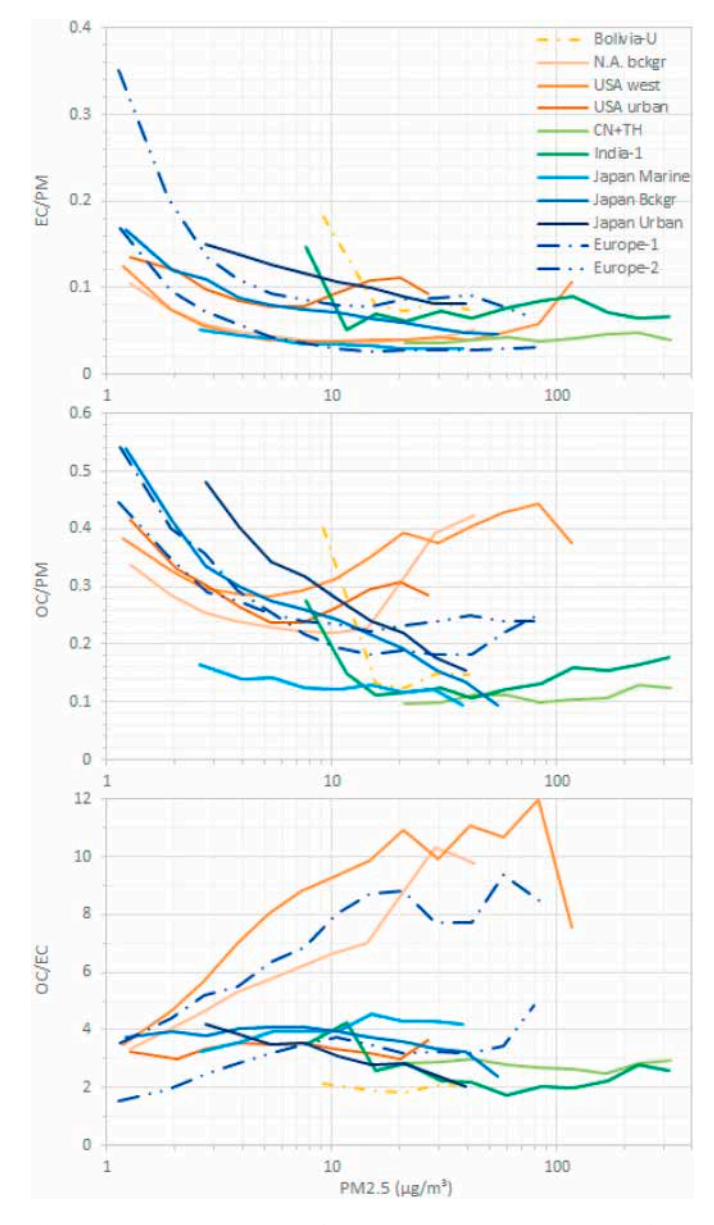


Fig. 23. Mean EC/PM, OC/PM and OC/EC ratios in $PM_{2.5}$ vs $PM_{2.5}$ mass for 11 groups of sites located in Latin America (Bolivia-U), North America (regional background in the western USA, in the remainder of the North America, and US urban sites), in China and Thailand, in India, Japan (marine, regional background, and urban sites), and in northern/western (Europe-1) and central/eastern Europe (Europe-2). OC and EC data from Europe (obtained with the EUSAAR_2 protocol) were converted to "IMPROVE_A equivalent" values.

DE, and Cabauw, NL (Fig. 17), EC/PM $_{10}$ ratios are lower compared with urban sites located in Latin America. Regarding Sahelian Africa, the EC/PM $_{10}$ vs. PM $_{10}$ curve falls between those for regional background sites in Europe and urban sites in Bolivia, with EC/PM $_{10}$ ratios averaging 0.01 over the PM $_{10}$ range of 30–50 µg/m 3 . Higher EC/PM $_{10}$ ratios were observed at other sites in Africa (Fig. 2, Table 4). Data from Thailand indicates slightly higher EC/PM $_{10}$ ratios (0.02) than those in the Sahel for PM $_{10}$ between 30 and 50 µg/m 3 . However, the two curves diverge for higher PM $_{10}$ mass concentrations, and for PM $_{10}$ > 100 µg/m 3 , EC/PM $_{10}$ ratios in Thailand are 5–10 times higher than those in the Sahel (Fig. 24), but remain similar to the EC/PM $_{10}$ ratio in Lamto, CI, in the forest-savannah transition zone (Fig. 2). For PM $_{10}$ mass between 30 and 50 µg/m 3 , EC/PM $_{10}$ ratios are higher in Seoul, KR, than in Thailand (Table 4), possibly due to higher contributions from uncontrolled diesel engine emissions compared to other PM $_{10}$ sources at this urban site.

Notably, EC/PM $_{10}$ ratios at Anmyeon-do Is., KR, are not lower than in Europe or the Sahel (Table 4).

Between Sahelian Africa, regional background sites in Europe, and urban sites in Bolivia, OC/PM $_{10}$ ratios are not as different as EC/PM $_{10}$ ratios are in the overlapping PM $_{10}$ concentration ranges (30 - 50 $\mu g/m^3$), with OC/PM $_{10}$ ratios averaging 0.07, 0.11 and 0.12, respectively. As for EC/PM $_{10}$ ratios, significantly higher OC/PM $_{10}$ ratios are observed at a number of sites in Latin America (Fig. 5) and Africa (Fig. 2, Table 4). OC/PM $_{10}$ ratios in the Sahel and Thailand are also similar in the range 40 < PM $_{10}$ < 80 $\mu g/m^3$ (0.05–0.06), but diverge beyond (Fig. 24). Higher OC/PM $_{10}$ ratios were observed at MEL, DE, in Europe for PM $_{10}$ concentrations greater than 60 $\mu g/m^3$ (Fig. 17).

The highest PM₁₀ OC/EC ratios are observed in Europe, at least for PM_{10} mass above 10 μ g/m³ (Fig. 24, Table 4). High $PM_{2.5}$ OC/EC ratios were also highlighted in western and northern Europe (Europe-1), and at regional background sites in North America (N.A. bckgr, US west) (Fig. 23, Table 3). This could be attributed to SOA and/or the condensation of semi-volatile organics contributing to the highest PM concentrations observed in Europe in summer and winter, respectively. Similarly high OC/EC ratios are observed at Chacaltaya, BO, in both PM₁₀ and PM₂₅, consistent with a dominant long-range transport of aged aerosol at this high-altitude site (Moreno et al., 2024). In Thailand and the Sahel, OC/EC mean ratios across the 30–50 μg/m³ PM₁₀ range are ~4 and ~6, respectively, about half of that observed in Europe. As indicated in Table 4, the lowest OC/EC ratios occur in Seoul, KR, independently of data harmonization, Bogotá, CO, and Lamto, CI. This suggests the predominant contribution of primary emissions to carbonaceous species sources at these three sites.

4. Conclusions

Despite the underrepresentation of certain global regions and the possible absence of some relevant datasets, this compilation of OC and EC data in PM_{10} and $PM_{2.5}$ provides a unique insight into the regional and seasonal variability of the aerosol carbon content worldwide.

The analysis reveals that EC generally makes up 1-5~% of PM_{10} and 3-10~% of $PM_{2.5}$ for PM mass ranging from 10 to $100~\mu g/m^3$. Notably low EC/PM ratios (0.01–0.03) are observed in Sahelian Africa, in line with a high content of mineral dust in PM_{10} , and at regional background sites in Europe and marine sites in Japan, where the contribution of combustion sources is minimal. Conversely, high EC/PM ratios (\sim 0.1) are found in central and eastern Europe, and urban sites in South America, North America and Japan, which are more heavily influenced by combustion primary emissions. Within the $PM_{2.5}$ overlapping range, EC concentrations are lower in India and China than in central and eastern Europe and at urban sites in the USA and Japan. However, they reach higher values during extreme PM pollution episodes.

OC contributes more than EC, comprising ${\sim}5{\sim}15$ % of PM_{10} and ${\sim}10{\sim}40$ % of $PM_{2.5}.$ On average, OC/PM ratios are low (${\sim}0.06)$ in PM_{10} in Thailand and the Sahel, and in $PM_{2.5}$ at marine sites in Japan, as well as in China, and India (${\sim}0.12$). Low OC/PM ratios can result from high PM mineral dust or sea salt content, or the predominance of inorganic aerosols over organic aerosols. For $PM_{2.5} > 10~\mu g/m^3$, the highest OC/PM ratios (>0.25) are found in North America and central and eastern Europe. In these regions, where outstandingly high OC/EC ratios suggest major contributions of SOA or wildfires, particulate organic matter, which includes OC and other elements, can be the major constituent of both PM_{10} and $PM_{2.5}$. Notably, the highest OC concentrations observed in North America and Asia are similar.

Seasonal variability and dependence of the EC/PM, OC/PM, and OC/EC ratios on $PM_{2.5}$ or PM_{10} concentrations provide hints on the possible sources and impacts of PM air pollution. Low EC/PM $_{10}$ ratios during the dry season in Sahelian Africa and Bogotá, CO, suggest that EC emissions from prescribed vegetation fires are overcompensated by soil dust emissions. In contrast, low EC/PM $_{2.5}$ ratios from June to August in North America, Japan, and Europe, along with high OC/EC ratios between

Table 3 EC/PM, OC/PM and OC/EC ratios for $PM_{2.5}$ mass between 20 and 40 μ g/m³, unless specified otherwise (see footnotes). Bold indicates original (unconverted) values.

			EC/PM			OC/PM			OC/EC		
			EUSAAR_2 T	IMPROVE_A R	NIOSH T	EUSAAR_2 T	IMPROVE_A R	NIOSH T	EUSAAR_2 T	IMPROVE_A R	NIOSH T
Caribbean	US Virgin Is ^(a)		0.01	0.01		0.05	0.04		6.6	4.6	
Latin America	Bolivia	urban	0.06	0.08		0.16	0.14		2.9	2.0	
North America	western USA	regional bckgr	0.03	0.04		0.43	0.39		14.9	10.5	
	other areas in N.A.	regional bckgr	0.03	0.04		0.40	0.36		13.6	9.6	
	USA	urban	0.08	0.11		0.35	0.31		4.6	3.2	
	Tahoe Lake		0.04	0.05		0.45	0.40		12.6	8.9	
	Simeonof Is(b)		0.03	0.04		0.31	0.27		15.9	11.1	
Asia	China + Thailand		0.03	0.04		0.11	0.10		4.2	2.9	
	Bangkok (TH) ^(c)		0.02	0.02		0.03	0.03		1.9	1.3	
	India-1		0.05	0.07		0.13	0.12		3.3	2.3	
	Bhopal (IN)		0.03	0.04		0.18	0.16		11.5	8.1	
	Darjeeling (IN)		0.12	0.12	0.09	0.35	0.35	0.40	2.8	2.9	4.3
	Delhi (IN) ^(d)		0.06	0.06	0.05	0.20	0.20	0.23	3.3	3.4	5.0
	Mohali (IN)		0.19	0.25		0.23	0.21		1.4	1.0	
	Mysuru (IN)		0.05	0.06		0.15	0.14		4.9	3.4	
	Srinagar (IN)		0.09	0.11		0.35	0.31		4.4	3.1	
	Japan	marine	0.02	0.03		0.13	0.12		5.8	4.0	
	Japan	regional bckgr	0.04	0.06		0.19	0.17		4.9	3.4	
	Japan	urban	0.07	0.08		0.22	0.20		3.7	2.6	
	Baengnyeong Is (KR))	0.03	0.04		0.12	0.10		4.1	2.9	
Europe	western + northern	regional bckgr	0.02	0.03		0.21	0.19		11.7	8.2	
	central + eastern	regional bckgr	0.05	0.07		0.28	0.25		6.4	4.5	

⁽a) PM2.5 range = 12–40 $\mu g/m$.

June and September, are consistent with a combination of reduced EC emissions related to domestic heating shutdown, and heightened SOA formation or OC-enriched wildfire emissions during summer in temperate climate zones. In China, India, and Thailand, the seasonal variations in EC/PM and OC/PM are influenced by open biomass burning, which diminishes during the wet summer monsoon season. However, domestic heating in winter can also contribute in regions where it is practiced. The relationships between the EC/PM and OC/PM ratios and PM mass indicate that OC and EC containing particles are less efficiently removed than others when PM concentrations drop below 10–15 μg/m³ due to e.g. pollution dispersion or wet removal, probably because of their lower hygroscopicity. The OC and EC contents of PM_{2.5} and PM₁₀ at high mass concentrations (PM > 40 μ g/m³) confirm that wildfires and agricultural waste burning drive PM pollution episodes at background sites in the western USA and large parts of Asia (China, India, Thailand), respectively. In western and northern Europe, higher PM concentrations are associated with higher OC/EC ratios, pointing to OC and OC precursor sources, including biomass burning for residential heating, as major contributors to PM air pollution.

These conclusions were drawn from datasets considered representative of specific locations, covering various periods between 2012 and 2019. The information in this study can be used for diagnosing or validating atmospheric chemistry models, taking into account that mass concentrations and compositions may have changed with time due to enforced regulation implementation and changing impacts of forest fires and/or dust storms (Ahangar et al., 2021; Altuwayjiri et al., 2021; Borlaza et al., 2022; Chow et al., 2022; Hand et al., 2019; Kim et al., 2020; Liu et al., 2024; Wang et al., 2022; Yttri et al., 2021; Yu et al.; Zhong et al., 2021). No data were found for Antarctica, Oceania, and extensive areas of northern and western Asia, while a few limited datasets only were available from Africa and South America. To support more comprehensive and up-to-date future assessments, atmospheric

observation programs are encouraged to persist in measuring EC, OC, PM and other aerosol variables following recommended protocols, and to make their data publicly available through open repositories like the World Data Center for Aerosols under the WMO/GAW program.

CRediT authorship contribution statement

Jean-Philippe Putaud: Writing – review & editing, Writing – original draft, Visualization, Methodology, Investigation, Formal analysis, Conceptualization. Fabrizia Cavalli: Investigation, Formal analysis. Karl Espen Yttri: Writing - review & editing, Investigation, Data curation, Writing - original draft. Judith C. Chow: Writing - review & editing, Data curation, Formal analysis, Methodology, Validation. John G. Watson: Writing - review & editing, Writing - original draft, Investigation, Data curation, Methodology. Baerbel Sinha: Writing review & editing, Investigation, Data curation, Project administration, Supervision, Validation. Chandra Venkataraman: Writing – review & editing, Data curation, Resources. Fumikazu Ikemori: Investigation, Data curation. Jean-Luc Jaffrezo: Writing - review & editing, Investigation, Funding acquisition, Project administration, Resources. Gaelle Uzu: Writing - review & editing, Investigation, Funding acquisition, Resources, Validation. Isabel Moreno: Writing - review & editing, Data curation, Writing - original draft. Radovan Krejci: Writing - review & editing, Investigation. Paolo Laj: Conceptualization, Writing – review & editing. Tarun Gupta: Conceptualization, Writing – review & editing. Min Hu: Conceptualization. Sang-Woo Kim: Visualization, Conceptualization, Data curation, Funding acquisition, Writing - review & editing. Olga Mayol-Bracero: Conceptualization, Investigation, Writing review & editing. Patricia Quinn: Conceptualization. Wenche Aas: Data curation, Writing – original draft. Andres Alastuey: Investigation, Data curation, Resources. Marcos Andrade: Investigation, Project administration. Monica Angelucci: Investigation, Formal analysis, Data

⁽b) PM2.5 range = $8-40 \mu g/m$.³.

⁽c) PM2.5 range = $20-45 \mu g/m.^3$.

⁽d) PM2.5 range = $20-75 \mu g/m$.³.

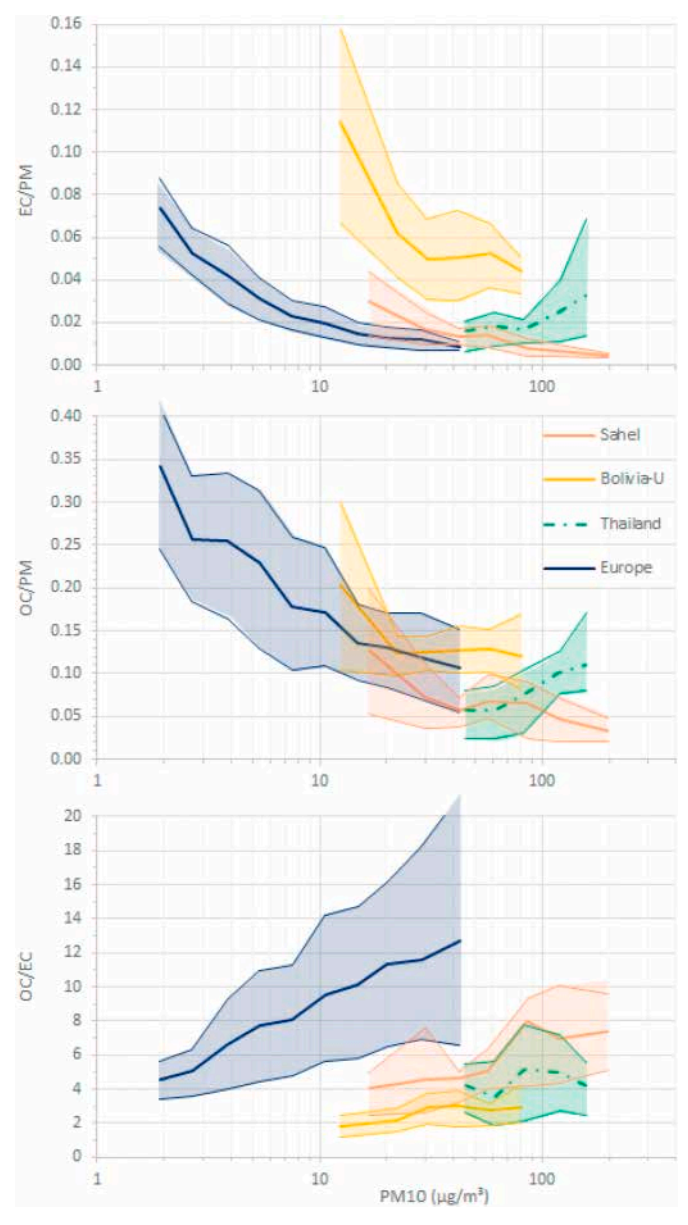


Fig. 24. Mean EC/PM, OC/PM and OC/EC ratios in PM₁₀ vs PM₁₀ mass for 4 groups of sites located in Africa, Bolivia, Thailand, and Europe. OC and EC data from Thailand (obtained with the IMPROVE_A protocol) were converted to "EUSAAR 2 equivalent" values.

curation. Gupta Anurag: Investigation, Formal analysis. Paul Beukes: Data curation, Funding acquisition, Project administration, Resources, Supervision, Writing - review & editing. Ankur Bhardwaj: Investigation, Formal analysis, Data curation. Abhijit Chatterjee: Data curation, Funding acquisition. Pooja Chaudhary: Investigation, Data curation. Anil Kumar Chhangani: Investigation. Sébastien Conil: Investigation, Data curation, Funding acquisition. Anna Degorska: Investigation. Sandeep Devaliva: Investigation, Abisheg Dhandapani: Investigation, Data curation. Sandeep Singh Duhan: Investigation. Umesh Chandra Dumka: Investigation, Data curation, Writing - review & editing. Gazala Habib: Investigation, Data curation, Formal analysis, Funding acquisition, Supervision. Zahra Hamzavi: Investigation. Diksha Haswani: Investigation. Hartmut Herrmann: Funding acquisition, Project administration, Resources, Supervision, Writing - review & editing. Adela Holubova: Data curation, Funding acquisition, Project administration, Writing - review & editing. Christoph Hueglin: Writing - review & editing, Data curation, Funding acquisition. Mohd Imran: Investigation. Arshid Jehangir: Writing - review & editing, Investigation, Data curation, Funding acquisition, Supervision. Taveen Singh Kapoor: Investigation. Angeliki Karanasiou: Investigation, Formal analysis, Writing – review & editing. Ravindra Khaiwal: Investigation, Data curation, Formal analysis, Methodology, Validation, Writing - review & editing. Jeongeun Kim: Data curation. Tanja Kolesa: Investigation. Joanna Kozakiewicz: Data curation. Irena Kranjc: Investigation. Jitender Singh Laura: Investigation. Yang Lian: Investigation, Resources. Junwen Liu: Investigation, Resources. Pooja Manwani: Investigation. Valeria Mardonez-Balderrama: Data curation. Béatrice Marticorena: Investigation. Atsushi Matsuki: Investigation, Data curation. Suman Mor: Investigation, Data curation, Formal analysis, Methodology, Validation, Writing - review & editing. Sauryadeep Mukherjee: Investigation. Sadashiva Murthy: Investigation, Data curation. Akila Muthalagu: Investigation. Tanveer Ahmad Najar: Investigation, Data curation, Formal analysis, Writing - review & editing. Radhakrishnan Naresh Kumar: Investigation, Project administration, Supervision, Validation. Govindan Pandithurai: Data curation, Funding acquisition, Project administration, Writing - review & editing. Noemi Perez: Investigation, Data curation. Worradorn Phairuang: Investigation, Methodology, Resources, Validation, Writing - review & editing. Harish C. Phuleria: Investigation, Methodology, Validation, Writing - review & editing. Laurent Poulain: Writing review & editing, Investigation, Formal analysis, Supervision, Validation. Laxmi Prasad: Investigation. Delwin Pullokaran: Investigation, Data curation. Adnan Mateen Qadri: Writing - review & editing. Asif Qureshi: Investigation. Omar Ramírez: Investigation, Formal analysis, Writing - review & editing. Sayantee Roy: Data curation, Formal analysis. Julian Rüdiger: Investigation, Formal analysis, Data curation. Binoy K. Saikia: Investigation, Writing - review & editing. Prasenjit Saikia: Investigation, Formal analysis, Methodology, Resources,

Table 4 EC/PM $_{10}$, OC/PM $_{10}$ and OC/EC ratio values for PM $_{10}$ mass concentrations between 30 and 50 μ g/m 3 . Bold indicates original (unconverted) values.

			EC/PM			OC/PM			OC/EC		
			EUSAAR_2 T	IMPROVE_A R	NIOSH T	EUSAAR_2 T	IMPROVE_A R	NIOSH T	EUSAAR_2 T	IMPROVE_A R	NIOSH T
	Sahel	regional bckgr	0.01	0.02		0.07	0.06		5.9	4.2	
	Lamto (CI)		0.05	0.06		0.21	0.18		4.1	2.9	
	Welgegund (ZA)		0.04	0.06		0.25	0.22		6.7	4.7	
Latin America	Bolivia	urban	0.05	0.06		0.12	0.10		2.79	2.0	
	Bogotá (CO)		0.10	0.12		0.26	0.23		3.4	2.4	
Asia Thailand		0.02	0.02		0.06	0.05		4.3	3.00		
	AMY (KR)	0.03	0.03	0.02	0.10	0.10	0.11	4.2	4.4	6.40	
	SEO (KR)		0.05	0.05	0.04	0.11	0.11	0.12	2.1	2.2	3.25
Europe	Europe	regional bckgr	0.01	0.01		0.11	0.10		11.0	7.7	
	CYP (CY)		0.01	0.01		0.05	0.04		6.1	4.3	
	CBW (NL)		0.02	0.03		0.13	0.12		6.8	4.8	
	MEL (DE)		0.02	0.03		0.19	0.17		10.6	7.5	

Supervision, Validation, Writing – review & editing. Stéphane Sauvage: Investigation, Data curation. Chrysanthos Savvides: Writing – review & editing. Renuka Sharma: Investigation. Tanbir Singh: Investigation. Gyanesh Kumar Singh: Writing – review & editing. Ronald Spoor: Investigation, Data curation. Atul Kumar Srivastava: Investigation, Data curation, Formal analysis, Writing – review & editing. Ramya Sunder Raman: Investigation, Data curation, Project administration, Resources, Supervision, Validation, Writing – review & editing. Pieter Van Zyl: Data curation, Funding acquisition, Project administration, Resources, Supervision, Writing – review & editing. Marco Vecchiocattivi: Investigation, Formal analysis, Data curation. Céline Voiron: Formal analysis, Methodology. Jinyuan Xin: Investigation. Kajal Yadav: Investigation, Data curation.

Funding

This work was supported by the infrastructure projects ACTRIS (EU FP7; Grant no. 262254), ACTRIS-2 (EU H2020; Grant no. 654109), the ACTRIS-D BMBF projects (Grant no. 01LK2002A); the Ministry of Environment, Forest and Climate Change (MoEF&CC), Govt. of India, under the NCAP-COALESCE project (Grant 14/10/2014-CC (Vol. II)): the Council of Scientific and Industrial Research, Grant no. 13008/72/ 2019-CC, MoEF&CC, Govt. of India; the Department of Science & Technology (DST), IRHPA Project, (Grant IR/S2/PF.01/2011), Govt. of India; the Swiss Federal Office for the Environment (FOEN); the Japanese government program JICA-JST SATREPS (Grant no. JPMJSA2102); the Office of the Permanent Secretary, Ministry of Higher Education, Science, Research and Innovation, Thailand (Grant No. RGNS 63-253); Ministry of Science and Technology of China (No. 2022YFF0802501); the Guangdong Provincial General Colleges and Universities Innovation Team Project (Natural 2024KCXTD004); the Ministry of Education, Youth and Sports of the Czech Republic (ACTRIS-CZ, Grant LM2023030); the German Federal Ministry for the Environment, Nature Conservation, Nuclear Safety and Consumer Protection (Air Monitoring Network of the German Environment Agency); the Korea Meteorological Administration's Research and Development program "Development of Asian Dust and Haze Monitoring and Prediction Technology" under Grant KMA2018-00521; the National Research Foundation of Korea (NRF) grant funded by the Korea government (MSIT) (No. RS-2024-00354627); and the Norwegian Environment Agency (Grant No. 17078061). The manuscript has been co-authored by employees of Brookhaven Science Associates, LLC, under Contract DE-SC0012704 with support from the U. S. Department of Energy's Atmospheric System Research program.

Declaration of competing interest

The authors declare that they have no known competing financial interests or personal relationships that could have appeared to influence the work reported in this paper.

Acknowledgements

This study was initiated by the Scientific Advisory Group on Aerosols of the Global Atmosphere Watch Program of the World Meteorological Organization.

It was made possible by ACTRIS (Aerosol, Clouds and Trace Gases Research Infrastructure), COALESCE (Carbonaceous Aerosol Emissions, Source Apportionment and Climate Impacts), IMPROVE (Interagency Monitoring of Protected Visual Environments), and INDAAF (International Network to study Deposition and Atmospheric composition in Africa). It forms part of the output of the Biogeochemistry Research Infrastructure Platform (BIOGRIP) of the Department of Science and Innovation of South Africa, which supports the Welgegund station. Samples were collected within the framework of the "International Network to study Deposition and Atmospheric chemistry in Africa".

The views expressed in this document are solely those of the authors and do not necessarily reflect those of the Indian Ministry of Environment, Forest and Climate Change. The Ministry does not endorse any products or commercial services mentioned in this publication.

Appendix A. Supplementary data

Supplementary data to this article can be found online at https://doi.org/10.1016/j.atmosenv.2025.121338.

Data availability

Data available from open access archives or from a specific zenodo archive, as specified in the manuscript.

References

- Ahangar, F.E., Pakbin, P., Hasheminassab, S., Epstein, S.A., Li, X., Polidori, A., Low, Jason, 2021. Long-term trends of PM2.5 and its carbon content in the South Coast Air Basin: a focus on the impact of wildfires. Atmos. Environ. 255. 118431.
- Amoako, E.E., Gambiza, J., 2021. Effects of fire on the population structure and abundance of Anogeissus leiocarpa and Vitellaria paradoxa in a West African savanna parkland. Acta Oecol. 112, 103745. https://doi.org/10.1016/j. actao 2021 103745
- Altuwayjiri, A., Pirhadi, M., Taghvaee, S., Sioutas, C., 2021. Long-term trends in the contribution of PM2.5 sources to organic carbon (OC) in the Los Angeles basin and the effect of PM emission regulations. Faraday Discuss 226, 74–99.
- Atkinson, R.W., Kang, S., Anderson, H.R., Mills, I.C., Walton, H.A., 2014. Epidemiological time series studies of PM2.5 and daily mortality and hospital admissions: a systematic review and meta-analysis. Thorax 69, 660–665. https://doi. org/10.1136/thoraxjnl-2013-204492 [Review].
- Bautista, A.T., Pabroa, P.C.B., Santos, F.L., Quirit, L.L., Asis, J.L.B., Dy, M.A.K., Martinez, J.P.G., 2015. Intercomparison between NIOSH, IMPROVE A, and EUSAAR 2 protocols: finding an optimal thermal-optical protocol for Philippines OC/EC samples. Atmos. Pollut. Res. 6, 334–342. https://doi.org/10.5094/ apr.2015.037.
- Beelen, R., Raaschou-Nielsen, O., Stafoggia, M., Andersen, Z.J., Weinmayr, G., Hoffmann, B., Wolf, K., Samoli, E., Fischer, P., Nieuwenhuijsen, M., Vineis, P., Xun, W.W., Katsouyanni, K., Dimakopoulou, K., Oudin, A., Forsberg, B., Modig, L., Havulinna, A.S., Lanki, T., Turunen, A., Oftedal, B., Nystad, W., Nafstad, P., De Faire, U., Pedersen, N.L., Ostenson, C.G., Fratiglioni, L., Penell, J., Korek, M., Pershagen, G., Eriksen, K.T., Overvad, K., Ellermann, T., Eeftens, M., Peeters, P.H., Meliefste, K., Wang, M., Bueno-De-Mesquita, B., Sugiri, D., Krämer, U., Heinrich, J., de Hoogh, K., Key, T., Peters, A., Hampel, R., Concin, H., Nagel, G., Ineichen, A., Schaffner, E., Probst-Hensch, N., Künzli, N., Schindler, C., Schikowski, T., Adam, M., Phuleria, H., Vilier, A., Clavel-Chapelon, F., Declercq, C., Grioni, S., Krogh, V., Tsai, M.Y., Ricceri, F., Sacerdote, C., Galassi, C., Migliore, E., Ranzi, A., Cesaroni, G., Badaloni, C., Forastiere, F., Tamayo, I., Amiano, P., Dorronsoro, M., Katsoulis, M., Trichopoulou, A., Brunekreef, B., Hoek, G., 2014. Effects of long-term exposure to air pollution on natural-cause mortality: an analysis of 22 European cohorts within the multicentre ESCAPE project. Lancet 383, 785–795. https://doi.org/10.1016/S0140-6736(13)0218-8.
- Bolton, J.L., Trush, M.A., Penning, T.M., Dryhurst, G., Monks, T.J., 2000. Role of quinones in toxicology. Chem. Res. Toxicol. 13 (3), 135–160. https://doi.org/ 10.1021/tx9902082.
- Borlaza, L.J., Weber, S., Marsal, A., Uzu, G., Jacob, V., Besombes, J.-L., Chatain, M., Conil, S., Jaffrezo, J.-L., 2022. Nine-year trends of PM₁₀ sources and oxidative potential in a rural background site in France. Atmos. Chem. Phys. 22, 8701–8723. https://doi.org/10.5194/acp-22-8701-2022.
- Bozzetti, C., Daellenbach, K.R., Hueglin, C., Fermo, P., Sciare, J., Kasper-Giebl, A., Mazar, Y., Abbaszade, G., El Kazzi, M., Gonzalez, R., Shuster-Meiseles, T., Flasch, M., Wolf, R., Křepelová, A., Canonaco, F., Schnelle-Kreis, J., Slowik, J.G., Zimmermann, R., Rudich, Y., Baltensperger, U., El Haddad, I., Prévôt, A.S., 2016. Size-resolved identification, characterization, and quantification of primary biological organic aerosol at a European rural site. Environ. Sci. Technol. 50 (7), 3425–3434. https://doi.org/10.1021/acs.est.5b05960. Epub 2016 Mar 15. Erratum in: Environ Sci Technol. 2016 Dec 6.,50(23):13177-3434. doi: 10.1021/acs. est.6b05500.
- Cavalli, F., Viana, M., Yttri, K.E., Genberg, J., Putaud, J.-P., 2010. Toward a standardised thermal-optical protocol for measuring. atmospheric organic and elemental carbon: the EUSAAR protocol. Atmos. Meas. Tech. 3, 79–89. https://doi.org/10.5194/amt-3-79-2010
- Chen, Y., Wang, H., Singh, B., Ma, P., Rasch, P.J., Bond, T.C., 2018. Investigating the linear dependence of direct and indirect radiative forcing on emission of carbonaceous aerosols in a global climate model. J. Geophys. Res. D. (Atmospheres) 123 (3), 1657–1672. https://doi.org/10.1002/2017JD027244. PNNL-SA-126780.
- Cheng, Y., He, K.-B., Duan, F.-K., Du, Z.-Y., Zheng, M., Ma, Y.-L., 2014. Ambient organic carbon to elemental carbon ratios: influence of the thermal–optical temperature protocol and implications. Sci. Total Environ. (468–469), 1103–1111. https://doi. org/10.1016/j.scitotenv.2013.08.084.

- Chow, J.C., Watson, J.G., Chen, L.-W.A., Arnott, W.P., Moosmüller, H., Fung, K.K., 2004. Equivalence of elemental carbon by Thermal/Optical Reflectance and Transmittance with different temperature protocols. Environ. Sci. Technol. 38, 4414–4422. https://doi.org/10.1021/es034936u.
- Chow, J.C., Watson, J.G., Chen, L.-W.A., Chang, M.C.O., Robinson, N.F., Trimble, D., Kohl, S.D., 2007. The IMPROVE A temperature protocol for thermal/optical carbon analysis: maintaining consistency with a long-term database. J. Air Waste Manage. Assoc. 57 (9), 1014–1023.
- Chow, J.C., Watson, J.G., Chen, L.-W.A., Rice, J., Frank, N.H., 2010. Quantification of PM_{2.5} organic carbon sampling artifacts in US networks. Atmos. Chem. Phys. 10, 5223–5239. https://doi.org/10.5194/acp-10-5223-2010.
- Chow, W.S., Liao, K.Z., Huang, X.H.H., Leung, K.F., Lau, A.K.H., Yu, J.Z., 2022. Measurement report: the 10-year trend of PM2.5 major components and source tracers from 2008 to 2017 in an urban site of Hong Kong. China. Atmos. Chem. Phys. 22, 11557 11572.
- EDGAR, v8.1, edgar.jrc.Ec.europa.eu/index.php/dataset_ap81, last accessed 31 October. 2024
- Fakhri, Y., Sarafraz, M., Javid, A., Moradi, M., Mehri, F., Nasiri, R., Saadatmandsepideh, S., 2024. The ratio of concentration of organic carbon and elemental carbon bound to particulate matter in ambient air: a global systematic review and meta-analysis. Int. J. Environ. Health Res. 10, 1–20. https://doi.org/ 10.1080/09603123.2024.2399207.
- Hallquist, M., Wenger, J.C., Baltensperger, U., Rudich, Y., Simpson, D., Claeys, M., Dommen, J., Donahue, N.M., George, C., Goldstein, A.H., Hamilton, J.F., Herrmann, H., Hoffmann, T., Iinuma, Y., Jang, M., Jenkin, M.E., Jimenez, J.L., Kiendler-Scharr, A., Maenhaut, W., McFiggans, G., Mentel, Th F., Monod, A., Prévôt, A.S.H., Seinfeld, J.H., Surratt, J.D., Szmigielski, R., Wildt, J., 2009. The formation, properties and impact of secondary organic aerosol: current and emerging issues. Atmos. Chem. Phys. 9, 5155–5236. https://doi.org/10.5194/acp-9-5155-2009.
- Hand, J.L., Prenni, A.J., Schichtel, B.A., Malm, W.C., Chow, J.C., 2019. Trends in remote PM2.5 residual mass across the United States: implications for aerosol mass reconstruction in the IMPROVE network. Atmos. Environ. 203, 141–152.
- Hang, Y., Meng, X., Xi, Y., Zhang, D., Lin, X., Liang, F., Tian, H., Li, T., Wang, T., Cao, J., Fu, Q., Dey, S., Li, S., Huang, K., Kan, H., Shi, X., Liu, Y., 2023. Environ. Res. Lett. 18, 124017. https://doi.org/10.1088/1748-9326/ad0862.
- Huang, H., Jin, Y., Sun, W., Gao, Y., Sun, P., Ding, W., 2024. Biomass burning in Northeast China over two decades: temporal trends and geographic patterns. Remote Sens. 16, 1911. https://doi.org/10.3390/rs16111911.
- Johnston, M.V., Kerecman, D.E., 2019. Molecular characterization of atmospheric organic aerosol by mass spectrometry. Annu. Rev. Anal. Chem. 12, 247–274. https://doi.org/10.1146/annurey-anchem-061516-045135.
- Kaly, F., Marticorena, B., Chatenet, B., Rajot, J.L., Janicot, S., Niang, A., Yahi, H., Thiria, S., Maman, A., Zakou, A., Coulibaly, B.S., Coulibaly, M., Koné, I., Traoré, S., Diallo, A., Ndiaye, T., 2015. Variability of mineral dust concentrations over west Africa monitored by the sahelian dust transect. Atmos. Res. 164–165, 226–241. https://doi.org/10.1016/j.atmosres.2015.05.011. ISSN 0169-8095.
- Karanasiou, A., Minguillón, M.C., Viana, M., Alastuey, A., Putaud, J.-P., Maenhaut, W., Panteliadis, P., Močnik, G., Favez, O., Kuhlbusch, T.A.J., 2015. Thermal-optical analysis for the measurement of elemental carbon (EC) and organic carbon (OC) in ambient air a literature review. Atmos. Meas. Tech. Discuss. 8, 9649–9712. https://doi.org/10.5194/amtd-8-9649-2015.
- Kelesidis, G.A., Neubauer, D., Fan, L.-S., Lohmann, U., Pratsinis, S.E., 2022. Enhanced light absorption and radiative forcing by black carbon agglomerates. Environ. Sci. Technol. 56 (12), 8610–8618. https://doi.org/10.1021/acs.est.2c00428.
- Kelly, J.M., Doherty, R.M., O'Connor, F.M., Mann, G.W., 2018. The impact of biogenic, anthropogenic, and biomass burning volatile organic compound emissions on regional and seasonal variations in secondary organic aerosol. Atmos. Chem. Phys. 18, 7393–7422. https://doi.org/10.5194/acp-18-7393-2018.
- Kim, Y., Yi, S.M., Heo, J., 2020. Fifteen-year trends in carbon species and PM2.5 in Seoul, South Korea (2003-2017). Chemosphere 261, 11. https://doi.org/10.1016/j. chemosphere.2020.127750.
- Kouassi, A., Doumbia, M., Silue, S., Yao, E., Dajuma, A., Adon, M., Touré, N., Yoboue, V., 2021. Measurement of atmospheric black carbon concentration in rural and urban environments: cases of Lamto and abidjan. J. Environ. Protect. 12, 855–872. https:// doi.org/10.4236/jep.2021.1211050.
- Kuwabara, H., Sekiguchi, K., Sankoda, K., Sakurai, K., Yamaguchi, R., Furuuchi, M., Hata, M., 2016. Evaluation of artifacts generated during collection of ultrafine particles using an inertial filter sampler. Aerosol Air Qual. Res. 16, 3063–3074. https://doi.org/10.4209/aagr.2015.12.0679.
- Lee, H., Honda, Y., Hashizume, M., Guo, Y.L., Wu, C.F., Kan, H., Jung, K., Lim, Y.H., Yi, S., Kim, H., 2015. Short-term exposure to fine and coarse particles and mortality: a multicity time-series study in East Asia. Environ. Pollut. 207, 43–51. https://doi.org/10.1016/j.envpol.2015.08.036.
- Leon-Marcos, A., Zeising, M., van Pinxteren, M., Zeppenfeld, S., Bracher, A., Barbaro, E., Engel, A., Feltracco, M., Tegen, I., Heinold, B., 2024. Modelling Emission and Transport of Key Components of Primary Marine Organic Aerosol Using the Global Aerosol-Climate Model ECHAM6.3—HAM2.3. EGUsphere. https://doi.org/10.5194/egusphere-2024-2917 [preprint].
- Lewtas, J., 2007. Air pollution combustion emissions: characterization of causative agents and mechanisms associated with cancer, reproductive, and cardiovascular effects. Mutta. Res. 636 (1–3), 95–133. https://doi.org/10.1016/j.
- Li, T., Yu, Y., Sun, Z., Duan, J., 2022. A comprehensive understanding of ambient particulate matter and its components on the adverse health effects based from

- epidemiological and laboratory evidence. Part. Fibre Toxicol. 19 (67). https://doi.org/10.1186/s12989-022-00507-5.
- Liu, Y., Xu, X., Ji, D., He, J., Wang, Y., 2024. Examining trends and variability of PM2.5-associated organic and elemental carbon in the megacity of Beijing, China: insight from decadal continuous in-situ hourly observations. Sci. Total Environ. 938, 173331. https://doi.org/10.1016/j.scitotenv.2024.173331.
- Lohman, U., Friebel, F., Kanji, Z.A., Mahrt, F., Mensah, A.A., Neubauer, D., 2020. Future warming exacerbated by aged-soot effect on cloud formation. Nat. Geosci. 13, 674–680. https://doi.org/10.1038/s41561-020-0631-0.
- Mahowald, N.M., Li, L., Vira, J., Prank, M., Hamilton, D.S., Matsui, H., Miller, R.L., Lu, L., Akyuz, E., Meidan, D., Hess, P., Lihavainen, H., Wiedinmyer, C., Hand, J., Alaimo, M. G., Alves, C., Alastuey, A., Artaxo, P., Barreto, A., Barraza, F., Becagli, S., Calzolai, G., Chellam, S., Chen, Y., Chuang, P., Cohen, D.D., Colombi, C., Diapouli, E., Dongarra, G., Eleftheriadis, K., Galy-Lacaux, C., Gaston, C., Gomez, D., González Ramos, Y., Hakola, H., Harrison, R.M., Heyes, C., Herut, B., Hopke, P., Hüglin, C., Kanakidou, M., Kertesz, Z., Klimont, Z., Kyllönen, K., Lambert, F., Liu, X., Losno, R., Lucarelli, F., Maenhaut, W., Marticorena, B., Martin, R.V., Mihalopoulos, N., Morera-Gomez, Y., Paytan, A., Prospero, J., Rodríguez, S., Smichowski, P., Varrica, D., Walsh, B., Weagle, C., Zhao, X., 2024. AERO-MAP: a data compilation and modelling approach to understand the fine and coarse mode aerosol composition. Earth Syst. Sci. Data Discuss. https://doi.org/10.5194/egusphere-2024-1617 [preprint].
- Maimone, F., Turpin, B.J., Solomon, P., Meng, Q., Robinson, A.L., Subramanian, R., Polidori, A., 2011. Correction methods for organic carbon artifacts when using quartz-fiber filters in large particulate matter monitoring networks: the regression method and other options. J. Air Waste Manag. Assoc. 61 (6), 696–710. https://doi. org/10.3155/1047-3289.61.6.696.
- Mardoñez, V., Pandolfi, M., Borlaza, L. Joanna S., Jaffrezo, J.-L., Alastuey, A., Besombes, J.-L., Moreno R, I., Perez, N., Močnik, G., Ginot, P., Krejci, R., Chrastny, V., Wiedensohler, A., Laj, P., Andrade, M., Uzu, G., 2023. Source apportionment study on particulate air pollution in two high-altitude Bolivian cities: La Paz and El Alto. Atmos. Chem. Phys. 23, 10325–10347. https://doi.org/10.5194/acp-23-10325-2023.
- Marticorena, B., Chatenet, B., Rajot, J.L., Bergametti, G., Deroubaix, A., Vincent, J., Kouoi, A., Schmechtig, C., Coulibaly, M., Diallo, A., Koné, I., Maman, A., Ndiaye, T., Zakou, A., 2017. Mineral dust over west and central Sahel: seasonal patterns of dry and wet deposition fluxes from a pluriannual sampling (2006-2012). J. Geophys. Res. Atmos. 122, 1338–1364. https://doi.org/10.1002/2016/JD025995.
- Moreno, C.I., Krejci, R., Jaffrezo, J.-L., Uzu, G., Alastuey, A., Andrade, M.F., Mardóñez, V., Koenig, A.M., Aliaga, D., Mohr, C., Ticona, L., Velarde, F., Blacutt, L., Forno, R., Whiteman, D.N., Wiedensohler, A., Ginot, P., Laj, P., 2024. Tropical tropospheric aerosol sources and chemical composition observed at high altitude in the Bolivian Andes. Atmos. Chem. Phys. 24, 2837–2860. https://doi.org/10.5194/acp-24-2837-2024.
- Ossohou, M., Galy-Lacaux, C., Yoboué, V., Hickman, J.E., Gardrat, E., Adon, M., Darras, S., Laouali, D., Akpo, A., Ouafo, M., Diop, B., Opepa, C., 2019. Trends and seasonal variability of atmospheric NO₂ and HNO₃ concentrations across three major African biomes inferred from long-term series of ground-based and satellite measurements. Atmos. Environ. 207, 148–166. https://doi.org/10.1016/j.atmosenv.2019.03.027.
- Ouafo-Leumbe, M.-R., Galy-Lacaux, C., Liousse, C., Pont, V., Akpo, A., Doumbia, T., Gardrat, E., Zouiten, C., Sigha-Nkamdjou, L., Ekodeck, G.E., 2018. Chemical composition and sources of atmospheric aerosols at Djougou (Benin). Meteorol. Atmos. Phys. 130, 591–609. https://doi.org/10.1007/s00703-017-0538-5.
- Atmos. Phys. 130, 591–609. https://doi.org/10.1007/s00703-017-0538-5. Pai, D.S., Bandgar, A., Devi, S., Musale, M., Badwaik, M.R., Kundale, A.P., Gadgil, S., Mohapatra, M., Rajeevan, M., 2020. New normal dates of onset/progress and withdrawal of southwest monsoon over India. CRS Research Report. RR No.3/2020, Office of the head, Climate Research & Services, IMD, Pune- 411005 (India).
- Phairuang, W., Suwattiga, P., Chetiyanukornkul, T., Hongtieab, S., Limpaseni, W., Ikemori, F., Hata, M., Furuuchi, M., 2019. The influence of the open burning of agricultural biomass and forest fires in Thailand on the carbonaceous components in size-fractionated particles. Environ. Pollut. 247, 238–247. https://doi.org/10.1016/ j.envpol.2019.01.001.
- Peterson, M.R., Richards, M.H., 2002. Thermal-optical transmittance analysis for organic, elemental, carbonate, total carbon, and OCX2 in PM2.5 by the EPA/NIOSH method. In: Winegar, E.D., Tropp, R.J. (Eds.), Proceedings, Symposium on Air Quality Measurement Methods and Technology-2002. Air & Waste Management Association, Pittsburgh, PA, p. 83, 1-83-19.
- Querol, X., Alastuey, A., Viana, M., Moreno, T., Reche, C., Minguillón, M.C., Ripoll, A., Pandolfi, M., Amato, F., Karanasiou, A., Pérez, N., Pey, J., Cusack, M., Vázquez, R., Plana, F., Dall'Osto, M., de la Rosa, J., Sánchez de la Campa, A., Fernández-Camacho, R., Rodríguez, S., Pio, C., Alados-Arboledas, L., Titos, G., Artínano, B., Salvador, P., García Dos Santos, S., Fernández Patier, R., 2013. Variability of carbonaceous aerosols in remote, rural, urban and industrial environments in Spain: implications for air quality policy. Atmos. Chem. Phys. 13, 6185–6206. https://doi.org/10.5194/acp.13-6185-2013
- Ramírez, O., Sánchez de la Campa, A.M., Amato, F., Catacolí, R.A., Rojas, N.Y., De la Rosa, J., 2018. Chemical composition and source apportionment of PM₁₀ at an urban background site in a high altitude Latin American megacity (Bogotá, Colombia). Environ. Pollut. 233, 142–155. https://doi.org/10.1016/j.envpol.2017.10.045.
- Rincón-Riveros, J.M., Rincón-Caro, M.A., Sullivan, A.P., Mendez-Espinosa, J.F., Belalcazar, L.C., Quirama Aguilar, M., Morales Betancourt, R., 2020. Long-term brown carbon and smoke tracer observations in Bogotá, Colombia: association with medium-range transport of biomass burning plumes. Atmos. Chem. Phys. 20, 7459–7472. https://doi.org/10.5194/acp-20-7459-2020.

- Sahu, L.K., Kondo, Y., Miyazaki, Y., Pongkiatkul, P., Kim Oanh, N.T., 2011. Seasonal and diurnal variations of black carbon and organic carbon aerosols in Bangkok. J. Geophys. Res. 116, D15302. https://doi.org/10.1029/2010JD015563.
- Samaké, A., Bonin, A., Jaffrezo, J.-L., Taberlet, P., Weber, S., Uzu, G., Jacob, V., Conil, S., Martins, J.M.F., 2020. High levels of primary biogenic organic aerosols are driven by only a few plant-associated microbial taxa. Atmos. Chem. Phys. 20, 5609–5628. https://doi.org/10.5194/acp-20-5609-2020.
- Schtaufnagel, D.E., 2020. The Health Effects of Ultrafine Particles. https://doi.org/ 10.1038/s12276-020-0403-3.
- Shi, Y., Gong, S., Zang, S., Zhao, Y., Wang, W., Lv, Z., Matsunaga, T., Yamaguchi, Y., Bai, Y., 2021. High-resolution and multi-year estimation of emissions from open biomass burning in Northeast China during 2001–2017. J. Clean. Prod. 310. https:// doi.org/10.1016/j.jclepro.2021.127496.
- Shiraiwa, M., Selzle, K., Pöschl, U., 2012. Hazardous components and health effects of atmospheric aerosol particles: reactive oxygen species, soot, polycyclic aromatic compounds and allergenic proteins. Free Radic. Res. 46 (8), 927–939. https://doi. org/10.3109/10715762.2012.663084.
- Smith, D.W., 2018. In: Zalta, Edward N. (Ed.), Phenomenology", the Stanford Encyclopedia of Philosophy (Summer 2018 Edition) plato.stanford.edu/archives/sum2018/entries/ phenomenology. (Accessed 31 October 2024).
- Szopa, S., Naik, V., Adhikary, B., Artaxo, P., Beerntsen, T., Collins, W.D., Fuzzi, S., Gallardo, L., Kiendler-Scharr, A., Klimont, Z., Liao, H., Unger, N., Zanis, P., 2023. Short-lived climate Forcers. In: Climate Change 2021 the Physical Science Basis: Contribution to Working Group I to the Sixth Assessment Report of the Intergovernmental Panel on Climate Change, first ed. Cambridge University Press. https://doi.org/10.1017/9781009157896.
- Tang, R., Shang, J., Qiu, X., Gong, J., Xue, T., Zhu, T., 2024. Origin, structural characteristics, and health effects of atmospheric soot particles: a review. Curr. Pollut. Rep. https://doi.org/10.1007/s40726-024-00307-9.
- Thangavel, P., Park, D., Lee, Y.-C., 2022. Recent insights into particulate matter (PM_{2.5})-Mediated toxicity in humans: an overview. Int. J. Environ. Res. Publ. Health 19, 7511. https://doi.org/10.3390/ijerph19127511.
- Thornhill, G.D., Collins, W.J., Kramer, R.J., Olivié, D., Skeie, R.B., O'Connor, F.M., Abraham, N.L., Checa-Garcia, R., Bauer, S.E., Deushi, M., Emmons, L.K., Forster, P. M., Horowitz, L.W., Johnson, B., Keeble, J., Lamarque, J.-F., Michou, M., Mills, M.J., Mulcahy, J.P., Myhre, G., Nabat, P., Naik, V., Oshima, N., Schulz, M., Smith, C.J., Takemura, T., Tilmes, S., Wu, T., Zeng, G., Zhang, J., 2021. Effective radiative forcing from emissions of reactive gases and aerosols a multi-model comparison. Atmos. Chem. Phys. 21, 853–874. https://doi.org/10.5194/acp-21-853-2021.
- U.S. EPA (U.S. Environmental Protection Agency), 2019. Integrated Science Assessment for Particulate Matter. EPA-600/R-19-188. Research Triangle Park, NC, cfpub.epa. gov/ncea/isa/recordisplay.cfm?deid=347534.
- Venkataraman, C., Bhushan, M., Dey, S., Ganguly, D., Gupta, T., Habib, G., Kesakar, A., Phuleria, H., Sunder Raman, R., 2020. Indian network project on carbonaceous aerosol emissions, source apportionment and climate impacts (COALESCE). Bull. Am. Meteorol. Soc. 101, E1052–E1068. https://doi.org/10.1175/BAMS-D-19-0030.1.

- Venkataraman, C., Anand, A., Maji, S., Barman, N., Tiwari, D., Muduchuru, K., et al., 2024. Drivers of PM_{2.5} episodes and exceedance in India: a synthesis from the COALESCE network. J. Geophys. Res. Atmos. 129, e2024JD040834. https://doi.org/ 10.1029/2024JD040834.
- Waldén, J., Hillamo, R., Aurela, M., Makela, T., Laurila, S., 2010. Demonstration of the Equivalence of PM2.5 and PM10 Measurement Methods in Helsinki 2007-2008, 103 s. Finnish Meteorological Institute. Studies 3, Helsinki, expo.fmi.fi/aqes/public/PM_ Equivalence%20report%20Helsinki_2010.pdf.
- Wang, H., Zhang, L., Yao, X., Cheng, I., Dabek-Zlotorzynska, E., 2022. Identification of decadal trends and associated causes for organic and elemental carbon in PM2.5 at Canadian urban sites. Environ. Int. 159, 107031. https://doi.org/10.1016/j. envint.2021.107031.
- Watson, J.G., Chow, J.C., Chen, L.W.A., 2005. Summary of organic and elemental carbon/black carbon analysis methods and intercomparisons. Aerosol Air Qual. Res. 5, 65–102. https://doi.org/10.4209/aaqr.2005.06.0006.
- Watson, J.G., Chow, J.C., Chen, L.-W.A., 2009. Methods to assess carbonaceous aerosol sampling artifacts for IMPROVE and other long-term networks. J. Air Waste Manage. Assoc. 59 (8), 898–911.
- Yttri, et al., 2011. Source apportionment of the carbonaceous aerosol in Norway quantitative estimates based on ¹⁴C, thermal-optical and organic tracer analysis. Atmos. Chem. Phys. 11, 9375–9394.
- Yttri, K.E., Canonaco, F., Eckhardt, S., Evangeliou, N., Fiebig, M., Gundersen, H., Hjellbrekke, A.-G., Lund Myhre, C., Platt, S.M., Prévôt, A.S.H., Simpson, D., Solberg, S., Surratt, J., Tørseth, K., Uggerud, H., Vadset, M., Wan, X., Aas, W., 2021. Trends, composition, and sources of carbonaceous aerosol at the Birkenes Observatory, northern Europe, 2001–2018. Atmos. Chem. Phys. 21, 7149–7170. https://doi.org/10.5194/acp-21-7149-2021.
- Yu, H., Chang, Y., Cheng, L., Duan, Y., and Hu, J., Long-term Assessment of Primary and Secondary Organic Aerosols in Shanghai Megacity throughout China's Clean Air Actions since 2010, doi.org/10.5194/egusphere-2024-1488 (under review).
- Yubero, E., Galindo, N., Nicolás, J.F., Lucarelli, F., Calzolai, G., 2014. Carbonaceous aerosols at an industrial site in Southeastern Spain. Air Qual. Atmos. Health 7 (3), 263–271. https://doi.org/10.1007/s11869-013-0233-8.
- Zhang, Y., Favez, O., Canonaco, F., Liu, D., Močnik, G., Amodeo, T., Sciare, J., Prévôt, A. S.H., Gros, V., Albinet, A., 2018. Evidence of major secondary organic aerosol contribution to lensing effect black carbon absorption enhancement. npj Clim Atmos Sci 1, 47. https://doi.org/10.1038/s41612-018-0056-2.
- Zhang, A., Wang, Y., Zhang, Y., Weber, R.J., Song, Y., Ke, Z., Zou, Y., 2020. Modeling the global radiative effect of Brown carbon: a potentially larger heating source in the tropical free troposphere than black carbon. Atmos. Chem. Phys. 20 (4), 1901–1920. https://doi.org/10.5194/acp-21-7149-2021.
- Zhong, Y., Chen, J.W., Zhao, Q.B., Zhang, N., Feng, J.L., Fu, Q.Y., 2021. Temporal trends of the concentration and sources of secondary organic aerosols in PM2.5 in Shanghai during 2012 and 2018. Atmos. Environ. 261, 8. https://doi.org/10.1016/j. scitotenv.2024.173331.